MODELING AND PREDICTION OF RAIN INDUCED ATTENUATION ON GSM BSC RADIO LINK
(A CASE STUDY OF AIRTEL NETWORK IN KADUNA)

BY

ISMAIL ADEKUNLE IMRAN

DEPARTMENT OF ELECTRICAL AND COMPUTER ENGINEERING
FACULTY OF ENGINEERING
AHMADU BELLO UNIVERSITY, ZARIA
NIGERIA

APRIL, 2015

CHAPTER ONE

INTRODUCTION

In this chapter, the background to this research is introduced along with the dissertation overview, the methodology adopted and the significant of the study. The background explains the importance of communication link and the over bearing effect of rain on the link at frequencies above 10GHz.

1.1 Background

Much attention has recently been shown to the use of higher frequencies for terrestrial and satellite communication links for civil, military and mobile communication systems globally. The use of higher frequency band for communication systems is necessary for higher channel capacities and also to avoid the congestion in VHF and UHF bands. As the communication systems using higher frequencies are growing rapidly in tropical countries, there is an increasing need for the knowledge of propagation characteristics of microwave because atmospheric effects play a major role in the design of the microwave links operating at frequencies above 10 GHz.. Basically, communication links operating at these frequencies are severely affected by the presence of rain over the link path, more so, in the tropical regions because of the high intensity of rain. Raindrops absorb and scatter radio waves, leading to signal attenuation and reduction of the system availability and reliability. The severity of rain impairment increases with frequency and varies with regional locations. It is therefore very important to make accurate prediction for the rain induced attenuation when planning for both microwave and terrestrial line-of-sight link.

The method for the prediction of rain attenuation on microwave paths has been grouped into two classes: the empirical method which is predicted from pointrainfall rate, drop-size distribution and other relevant parameters along the radio paths or through link measurements, and the physical method which is an attempt to reproduce the physical behaviour involved in the attenuation process. However, when a physical approach is used not all the input parameters needed for the analysis are available. Empirical method is therefore the most used methodology largely from the point rainfall rate and dropsizes distribution data (Ojo et al 2008). For the use of the empirical method, an appropriate distribution of rainfall rate at 1-minute integration time is needed for the site under studies in order to have accurate rain attenuation prediction for the location. Studies have shown that there is still dearth of rainfall rate at 1-minute integration time for the prediction of rain attenuation because all national weather bureaus and environmental agencies in the tropical countries of the world only record daily or hourly rainfall data. Very important effort made towards gathering moreinformation on the 1-minute rain rate was through the use of distrometer or the Tropical Rain Measurement Mission (TRMM)jointly developed by the United States and Japan, and the GlobalPrecipitation Climatology Project (GPCP) of the World ClimaticResearch Programme (WCRP). The data available from this mission cannot directly be used in system design, due to its long integration time.A method for converting the available rain rate data to the equivalent 1-minute rain rate cumulative distribution is therefore necessary. Even though the International Telecommunication Union (ITU-R) provides the global model, most attempts for the 1-minute rain rate involved extrapolation of measurements from one

location to the other. However, the complex nature and regional variability of rain make this approach highly inaccurate.

Consequently, the need for local experimentally determined parameters such as the received signal level (RSL) of the microwave link cannot be ignoredfor the reliable communication system because it will provide the knowledge of the link fade margin to be provided in the system design in order to overcome the losses in the signal strength due to rain over the path.Therefore, this dissertation presents the modeling and prediction of rain induced attenuation using empirical approach from the measured received signal level (RSL) of BSC radio over a period of two rainy seasons in Kaduna.

1.2 Research Motivation

Microwave links are used extensively for base station backhaul in the base station subsystem of mobile communication network of GSM in Nigeria. At present, more than 60% of all base stations are connected via microwave links because the majority ofoperators (Airtel) seek to minimize their operating expenses (OPEX) by owning their own transport networks instead of leasing capacity. These communication links being used in the Abis interface of the GSM architecture operate at frequencies above 10GHz. The utilization of this higher frequency band provides a number of important benefits, it relieves the congestion in the lower frequency bands and it also exploits the larger bandwidths available at higher frequencies so as to accommodate the high demands for broadband services. Despite the advantages suggested by the use of these frequency bands, the systems can be easily degraded by some natural atmospheric phenomena of which rain is the principal factor and needs to be appropriately quantified so as to enhance reliable communication (Freeman, 1997). This is not to assume that other factors

such as crosstalk or inter-system interference have become irrelevant, but in a situation where the effect of rain is so severe that a communication links nolonger functions, then other factors can be considered as secondary. Rain being a natural phenomenon which displays a high degree of spatial and temporal variation along the signal propagation paths from location-to-location on yearly or monthly basis, causes substantial rain induced attenuation, which is a dominant impairment to successful delivery of both voice messages and data even with digital communication link at high frequency of propagation (Odedina et al, 2007).

There have been extensive works done on the measurement of rain drop size distributions, radar reflectivity and rain rate for the investigation of rain-induced impairment to radio signals at super high frequencies. Most of these works were carried out in the temperate regions. However, some researchers have carried out similar studies in tropical locations. Such studies include the measurement of rain drop size distributions at Ile-Ife by Olsen and Ajayi, (1999),Ajayi et al, (1999) at Ilorin, Zaria and Calabar using the disdrometer, while the measurement of rainfall intensity was done using rain gauge. Presently, there has not been any measurement of the vertical profile of rainfall parameters in Nigeria. Therefore, the need to provide empirical model using the measured received signal level (RSL) of link when there is rain drops on the antenna. It is believed that the approach uniqueness would account for the accurate profile of the rain effect on a microwave link in an area from the measured signal fade margin of the link.

1.3 Problem Statement

The effectiveness of wireless communication systems to a large extent depends on the transmission medium. Due to new needs and developments, system designers are interested in frequencies above 10 GHz. At these frequencies rain attenuation is one of the key parameters considered in link design and budgeting. For this reason, the International Telecommunication Union (ITU) recommends an expression for rain attenuation at a given frequency and rain rate (Seker and Kunter, 2013). Although this simple model (aR^b)is widely used in telecommunications, however,the model does not accurately account for rain induced attenuation everywhere in the world because the rain rate and drop size distribution changes and are different across the climatic regions of the world. Consequently, a modification of the ITU-R model is important based on the actual climatic condition of a region for a reliable design of microwave link.

1.4 Aim and Objectives

The aim of this research work is to develop an empirical model for the accurate prediction of rain induced attenuation at 13GHz and 15GHz frequencies using BSC microwave link of Airtel GSM network in Kaduna.

The objectives of this study are to:

(i) Conductperformance analysis of the digital microwave links used in the A_{bis}Interface of GSM network under the effect of raindrops.

(ii) Determine the links worst faded signal level due to rainfall

(iii) Determine the rain induced attenuation from the links Received Signal Level

(RSL) variation measurement on the 13GHz and 15GHz microwave links

(iv) Developempirical models for the accurate prediction of rain induced attenuation for microwave links based on the measured data

(v) Validate the developed models using the ITU-R model.

1.5 Methodology

Thisresearch is based on the direct measurement of the radio Received Signal Levels (RSL) as a unique radio propagation process, which could increase the accuracy of conventional propagation model predictions by making use of direct on-air link data. Toachieve this the following methodology was adopted:

(i) Collection of rain fall data from Nigeria meteorological Agency, (NIMET)

(ii) Determination of rain rate R_p from the NIMET data.

(iii) Direct measurement of RSL on the 13GHz and 15GHz microwave links during clear sky (when there is no rain or dust storm) and during heavy rainfall (April to October) for the years 2009 and 2010 respectively.

(iv) Development of empirical models using Lease Square Method based on items (ii) and (iii).

(v) Evaluation of the developed model using the following:

(a) Chi-Square Test;

(b) RMSE statistical analysis.

(vi) Simulation of the models usingMATLABSignal Processing tools boxR2008a to predict rain attenuation at 13GHz and 15GHz.

(vii) Validation of the developed model using the ITU-R model.

1.6 Significant Contributions

The following are some of the contributions achieved as an indication of the significance of this research work:

(i) Empirical models were developed for 13GHz and 15GHz microwave frequencies based on direct measurement of the link performance.The predicted models showed that the rain-induced attenuation is directly proportional to the rain rate.

(ii) The study showed that the ITU-R model under estimated rain induced attenuation at 13GHz and 15GHz frequencieswith mean error of 0.78 and 3.02dB respectively when compared with the developed models, and the model under estimation increases with rain rate and frequency increase.

(iii) The study also ascertained the links worst performance under heavy rain with signal fading of -77dBm and -80dBm for the 13GHz and 15GHz frequencies respectively and predictedexcess rain attenuation of 11.35dB at 13GHz and 18.78dB at 15GHz microwave frequencies. The ITU-R model cannot be used to determine the link signal fading.

1.7 Dissertation Outline

This dissertation is divided into five chapters. Each chapter gives a summary of what it contains. Chapter is an introduction that covers the background knowledge and motivation for this research work, the problem statement, aim and objectives, the dissertation overview and itscontributions to knowledge.

Chapter two deals with literature review, which included critical review of basic fundamental concepts of wave propagation and propagation losses, as well as various existing rain attenuation models, especially, the few developed for tropical regions of the world. Detailed descriptions of some rain attenuation investigations that have been carried out in different parts of the world were discussed. This is the descriptive part of the dissertationand is intendedto present a general overview of some experimental and theoretical terrestrial rain attenuation models that have been proposedby different authors. Rain rate statistics in theform of rain rate cumulative distributions was discussed here as the starting point of all rainattenuation prediction models. The theoretical approach for the calculation of rain attenuation along a terrestrialcommunication radio link based on the assumption that the raindrops are non homogenous was discussed in this chapter, including the principle of effective path length for path loss estimation by the different authors. Lastly, the chapter gives account of some similar research works carried out in this area keen emphasis on the model formulation approach, validation of the predicted models and the limitations.

Chapter three unveils the material and method, for the analysis data collected and measured. It explains how data processing and theoretical empirical modeling using least square method generates different curve fitting functions for the experimental data point with the help of Microsoft Excel toolbox. Also it covers the evaluation of these curve fitting functions by statistical techniques using Chi-Square Test and Root Mean Square Error (RMSE) and simulation of the chosen functions usingMATLAB R2008a signal processing toolbox, as well as their validation with the ITU-R model by

comparison.Chapter four gives detail analysis and discussion of the result obtained. Chapter five presents the conclusion and recommendations drawn from the study.

CHAPTER TWO

LITERATURE REVIEW

2.1 Introduction

In this chapter, a review of basic fundamental concepts relating to microwave propagation and propagation impairment was made, as well asthe choice of the different types of digital microwave link used in mobile telecommunication and the advantage of one over the other. The GSM architecture with interest in the network interfaces, especially the Um and the Abis physical interfaces which operate basically on radio frequency (RF) are highlighted here. Various propagation impairment and the attendant physical causes are presented with critical review of effects of rain drops on microwave propagation. The theoretical concept of the specific rain attenuation and the effect of 1-minute integration time for the formulation of rain induced attenuation model are also discussed. Terrestrial rain induced attenuation models developed by different authors for different terrains with their basic uniqueness are reviewed with the focus on the few with primary concern for the tropical regions of the world.Quite a numbers of similar research works on this topic are reviewed with critical analysis of their applications and limitations.

2.2 Review of Fundamental Concepts

Fundamental concepts relating to microwave propagation as well as the various impairments suffered by the signal are discussed with attention to the effects of raindrops on radio waves. Use of microwave link in the GSM system interface was also reviewed. Also discussed is the ITU-R study group theory on the global rain map regional classification, including the concept of specific rain attenuation:

2.2.1 Microwave Links

A microwave link is the wireless communications system via radio frequency (RF). Telecommunications operators usually employ microwave links like the Synchronous Digital Hierarchy, (SDH) and Plesiochronous Digital Hierarchy, (PDH) as backbone terrestrial communication systems for transporting large amounts of telephone calls and data traffic over the same fiber or microwave link without synchronization problem. The SDH was primarily designed for two reasons:

(i) To transport circuit mode communications (DS1 and DS3) from a variety of different sources.

(ii) To support real-time, uncompressed, circuit-switched voice encoded in PCM format (Ray, 2007)

These were difficult with PDH system because:

(i) The synchronization sources of the various circuits were different.

(ii) Each circuit was operating at a slightly different rate and with different phase (Ray, 2007).

Typically, microwave links are very suitable for very high bit rate systems and large

area coverage. Microwave links suffer from a variety of signal degradation. The presence of hydrometeors such as rain, fog, water vapor and oxygen in the radio wave path can produce significant effect in the energy absorption, especially for the microwave links that employ line-of-sight (LOS) propagation at 10GHz and above (Owolawi and Afullo,2007)

2.2.2 Line of sight (LOS) Microwave Link

“Line-of-sight" (LOS) is a term used in radio system design to describe a condition in which radio device antennas can actually see each other. High frequency radios, such as those used in spread spectrum require line-of-Sight between antennas (Odedina and Afullo, 2007)

A typical line-of-sight microwave link is shown in Figure 1.1 (Crane, 2003). It useshighly directional transmitting and receiving antennas to communicate via a narrowly focused radio beam. The transmission path of a line-of-sight microwave link can be established between two land-based antennas, between a land-based antenna and a satellite-based antenna, or between two satellite antennas. Broadband line-of-sight links operate at frequencies between 1 and 25 GHz and can have transmission bandwidths approaching 600MHz (Crane, 2003)

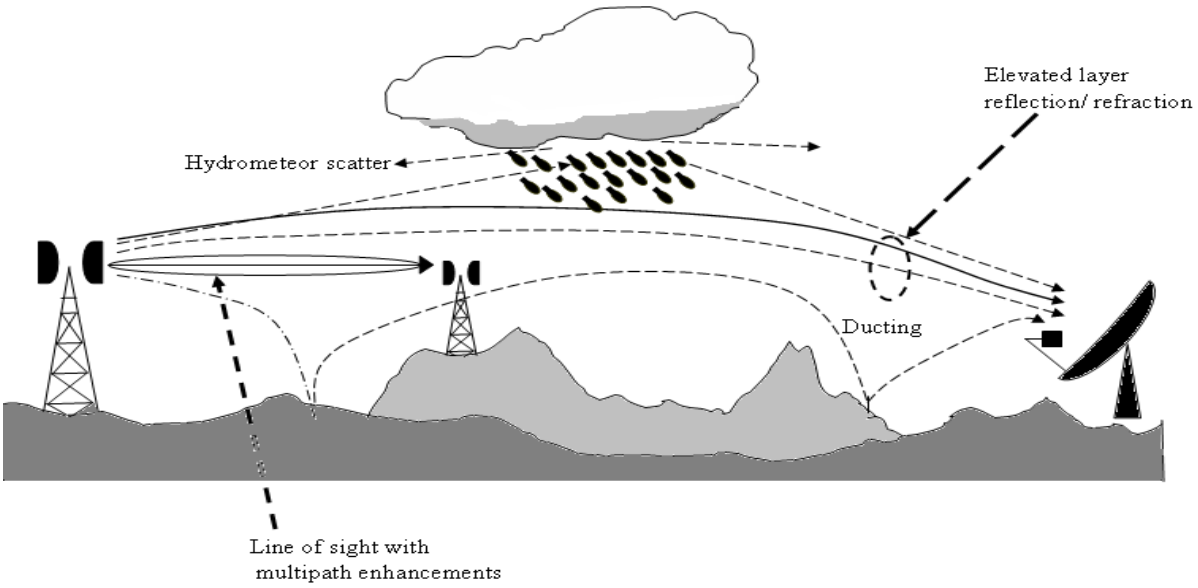

Figure 2.1: Line-of-Sight Antenna under Atmospheric Effect (Crane, 2003)

2.2.3 Global System for Mobile Communications (GSM)

GSM is a digital, mobile; radio standard developed for mobile, wireless, voice communications.GSM uses a combination of both the Time Division Multiple Access (TDMA) and Frequency Division Multiple Access (FDMA). With this combination, more channels of communications are available, and all channels are digital. The increase demand for large data, audio and video traffic has necessitated migration to Universal Mobile Telecommunication System, (UMTS). The important difference between mobile UMTS and GSM systems in terms of radio propagation is the difference in the carrier spacing, which is 5 MHz in UMTS systems and 200 kHz for GSM systems

The GSM service is available in the following frequency bands 900-MHz, 1800-MHz and 1900-MHz while the mobile UMTS which is a third generation network (3G) operates at 2100MHz and 2270MHz (Agile Technologies, 2000), GSM fundamentals.

2.2.3.1 GSM Network Elements

A generic GSM network interfaces is illustrated in Figure 1.2. The interface facilitates the information interchanges that take place within the network. It also enables the use of network elements from different manufacturers.

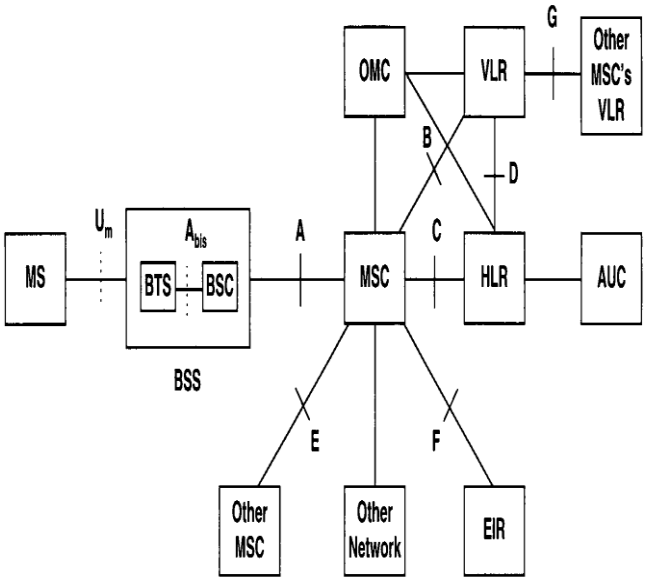

Legend

U_m: radio Interface
A_{bis}: radio Interface
A: Interface
B: Interface
C: Interface
D: Interface
E: Interface
F: Interface
G: Interface

Figure 2.2: Typical GSM Network Showing Key Interfaces (GSM Architecture and Interfaces1998)

2.2.3.2 GSM Interfaces

The network structure is defined within the GSM standards and each interface between the different elements of the GSM network is also defined. This facilitates the information interchanges that take place within the system. It also enables use of network elements from different manufacturers. The Interfaces include:

The Um interface also known as the "air" or radio interface standard that is used for exchanges between mobile equipment (ME) and a base station (BTS / BSC). For

signaling, a modified version of the integrated system of digital network (ISDN)Link Access Protocol on the D channel (LAPD), known as Link Access Protocol on the Dm channel (LAPDm) is used.(Radio-Electronics)

The A_{bis} interface is a base station subsystem (BSS) internal interface linking the base transceiver stations (BTS) and a base station controller (BSC), and it has not been totally standardized. The A_{bis} interface allows control of the radio equipment and radio frequency allocation in the BTS (Radio-Electronics).

The A interface used to provide communication between the base station subsystem (BSS) and the mobile service switching center (MSC). The interface carries information to enable the channels, timeslots and the like to be allocated to the mobile equipments being serviced by the BSSs. The messaging required within the network to enable handover etc to be undertaken is carried over the interface(Radio-Electronics).

The B interface exists between the mobile service switching center (MSC) and the visitor location register (VLR). It uses a protocol known as the MAP/B protocol. As most VLRs are collocated with an MSC, this makes the interface purely an "internal" interface. The interface is used whenever the MSC needs access to data regarding a MS located in its area(Radio-Electronics).

The C interface is located between the HLR and a GMSC or a SMS-G. When a call originates from outside the network, i.e. from the PSTN or another mobile network it has to pass through the gateway so that routing information required to complete the call may be gained. The protocol used for communication is MAP/C, the letter "C" indicating that the protocol is used for the "C" interface. In addition to this, the MSC may optionally

forward billing information to the HLR after the call is completed and cleared down (Radio-Electronics).

The D interface is situated between the VLR and HLR. It uses the MAP/D protocol to exchange the data related to the location of the ME and to the management of the subscriber (Radio-Electronics).

The E interface provides communication between two MSCs. The E interface exchanges data related to handover between the anchor and relay MSCs using the MAP/E protocol (Radio-Electronics).

The F interface is used between an MSC and EIR. It uses the MAP/F protocol. The communications along this interface are used to confirm the status of the IMEI of the ME gaining access to the network(Radio-Electronics).

The G interface interconnects two VLRs of different MSCs and uses the MAP/G protocol to transfer subscriber information, during e.g. a location update procedure.

In terms of the physical layer, the air interface (MS-BTS) uses RF radio transmission. The Abis interface (BTS-BSC) uses 64 kbps over whatever medium is most convenient for installation: wire, optical, or microwave. In this interface, Airtel network uses 64kbps over microwave links of 7.2GHz, 13GHz and 15GHz subject to the coverage distance required. Use of these microwave links at frequencies above 10GHz, informed the study of their performance considering propagation impairment like raindrops.All other interfaces in the GSM system use SS7/C7s MTP1 at the physical layer. The air interface (MS-BTS) and the A-bis interface (BTS-BSC) do not have a network layer. All other

interfaces in the GSM system use SS7/C7s MTP3 and SCCP at the network layer (Radio-Electronics).

2.2.4 Propagation Impairment on Radio Waves

Radio wave propagation is one of the most important phenomena in our daily lives. It is almost indispensible and without it our communication would be impaired. But, at the same time it is very complex. Numbers of inevitable factors affect the radio propagation as evaluated in Table 2.1,

Table 2.1: Effects of Various Atmospheric Factors on Radio Wave Propagation(Ashish and Prashant, 2010).

Propagation Impairment	Physical Cause	Prime Importance
Attenuation and sky noise increases	Atmospheric gases, cloud, rain.	Frequencies above 10 GHz
Signal Depolarization	Rain Ice crystals	Dual-polarization systems at C band and Ku- bands (depends on system configuration)
Reflection, Atmospheric multipath	Atmospheric gases	Communication & tracking at low elevation angles
Signal Scintillation	Tropospheric refractivity fluctuations	Troposheric at frequencies above 10GHz and low elevation angles
Reflection, Multipath and blockage	Earth's surface, objects on surface	Mobile satellite service
Propagation delay, variations	Troposphere	Precise timing and location systems, TDMA systems
Inter system interferences	Ducting, Scatter, diffraction	Mainly C- band at present, rain scatter may be significant at higher frequencies

In the above-mentioned factors, rain and water play a significant role in the attenuation of the radio waves propagations, (Ashish and Prashant, 2010).Propagation losses are key design parameters of concern in communication system. There are three propagation losses which include the free space losses, the atmospheric losses and the pointing losses.The focus is always on the atmospheric losses because it is derived from the absorption of energy by atmospheric gases. Atmospheric losses could be due to ionospheric or troposheric effects and variation from one geographical location to the other.All radio waves pass through the ionosphere, the highest layer of the atmosphere, which contains ionized particles due to the action of sun's radiation. Free electrons are distributed in layers and clouds of electrons may be formed, originating what is known as travelling ionospheric disturbances, which provoke signal fluctuations that are only treated as Polarization rotation; Scintillation effects; Propagation delay; or Dispersion effects. These effects decrease usually with the increase of the square of the frequency and the differences in the atmospheric refractive index may cause scattering and multipath effect, due to the different directions rays may take through the atmosphere. Table 2.1 showed the physical causes of this impairment including those due to tropospheric effects whichis composed by a miscellany of molecules of different compounds, such as hail, raindrops or other atmospheric gases. Radio waves that pass by troposphere will suffer their effects and will be scattered, depolarized, absorbed and therefore attenuated.

2.2.5 Effects of Rain on Radio Wave Propagation

The radio wave propagation is affected by rain in two forms, that is, radio signals are either scattered or absorbed by rain particles:

(a) Scattering of Radio Signals

Scattering of the radio signal into different direction by the rain droplets is known as rain scattering. This rain scattering is a function of the wavelength of the radio wave and the size of the scattering particle. Raindrops are not truly spherical, which results in differently polarized waves to suffer different attenuation (scattering and absorption by rain drops). Hence, rain scattering depends on the polarization of the radio waves. A horizontally polarized wave would be scattered forward or backward. In case of forward scattering, the propagation range increases by 800 km. A vertically polarized wave suffers sideway scattering (Ashish and Prashant, 2010).The scattered wave introduces unwanted or interfering signals into the communication receiver that may mask thedesired signal thereby causing attenuation (reduction of signal strength or power). Fig. 2.3 shows the scattering and the absorption effect of radio wave when it is incident on a rain-filled medium (Crane, 2003)

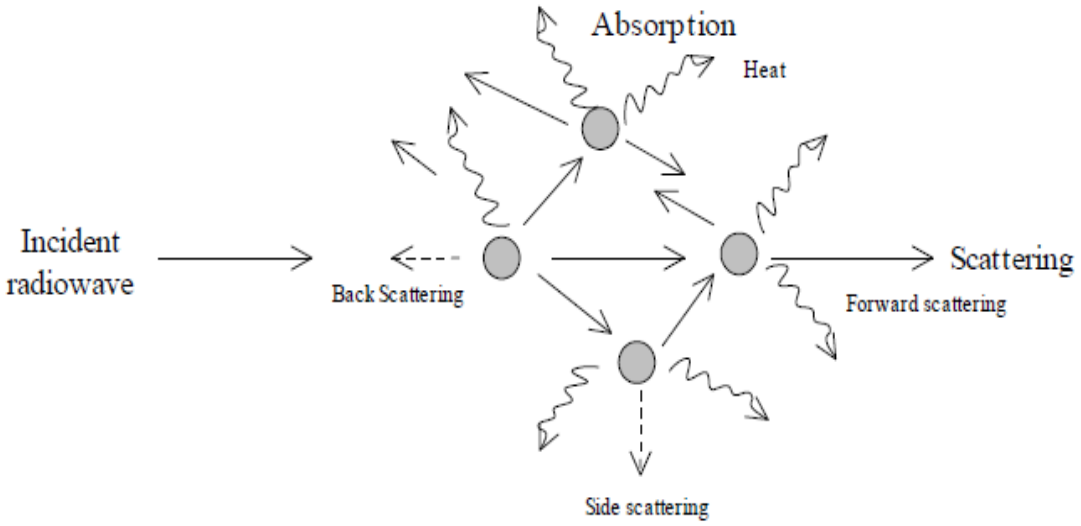

Figure 2.3: Scattering and Absorption of Radio Waves in a Rain-Filled Medium

Howscattered or absorbed the electromagnetic wave can be depends on the raindrop size,

shape andthe materials of which the raindrop is made up of (Moupfouma, 2009). The attenuationexperienced by a radio wave crossing a rainy medium is given by the sum of the individualcontributions of the drops that constitute the medium. Since rainfall consists of drops of variousdimensions, the specific attenuation is calculated by integrating each raindrop contribution.

(b) Absorption of Radio Signals

Rain plays a significant role in the undesired absorption of the radio wave in the lower atmosphere especially at microwave frequencies above 10GHz. Such absorption causes variation in signal strengths and hence, results in the attenuation of the signal. Rain Attenuation is a function of rain rate. Rain rate is the amount of precipitation occurring in a unit of time; generally expressed in millimeter per hour (mm/h). The main interest is the percentage of time that specified values of the rain exceeded. The time percentage is usually that of a year; for example, a rain rate of 0.001 percent means that the rain rate would be exceeded for 0.001 percent of a year or 5.3 min during any one year. In this case, the rain rate is denoted as $R_{0.001\%,}$ (Odedina and Afullo, 2007). In general the percentage time is denoted by p and the rain rate is denoted as R_p

2.2.6 ITU-R Study Group

The International Telecommunication Union, Radio communication (ITU-R) study group has developed point rain-rate distribution models for the prediction of cumulative distributions of rain attenuation on terrestrial line-of-sight links since early 1970's (Olsen and Ajayi, 1999). This was done so as to provide information needed for the prediction of rain attenuation for all locations on the globe especially for regions without adequate rain data (Ajayi et al., 1999). This model initially divided the whole globe into fifteen discrete

rain zones by using median cumulative distribution of rain rate for the rain climatic region.

Table 2.2: ITU-R Rain Climatic Regions (ITU-R 837-4, 2007)

Percentage time Rain exceeded	Regions														
	A	B	C	D	E	F	G	H	J	K	L	M	N	P	Q
1.0	<0.1	0.5	0.7	2.1	0.6	1.7	3	2	8	1.5	2	4	5	12	24
0.3	0.8	2	2.8	4.5	2.4	4.5	7	4	13	4.2	7	11	15	34	49
0.1	2	3	5	8	6	8	12	10	20	12	15	22	35	65	72
0.03	5	6	9	13	12	15	20	18	28	23	33	40	65	105	96
0.01	8	12	15	19	22	28	30	32	35	42	60	63	95	145	115
0.003	14	21	26	29	41	54	45	55	45	70	105	95	140	200	142
0.001	22	32	42	42	70	78	65	83	55	100	150	120	180	250	170

ITU-R determined the rain rate exceeded for different percentages of time into fifteen climatic rain zones ranging from A to Q as shown in Table 2.2 and Appendix 2B (ITU-R 837-4, 2007). From the ITU-R Table, Nigeria was categorized to the P region of the ITU-R African rain map with $R_{0.01\%}$ of 145mm/h. Due to the discrete nature of the zonal approach in the ITU-R rain climatic zone and its inherent lack of precision to some degree in some climatic rain zones in their initial classification, other attempts have been made to predict point rain rate distributions at specific points within a region (Olsen,

1999). Some of these approaches have used measured rain rate distributions for as many locations in a region as possible, and then fitted into contour maps for particular parameters of the distribution. The contour maps produced by this approach have been regularly revised and updated by the radio communication study groups of the ITU (see Appendix 2B). More recently, the ITU-R (ITU-R 837-4, 2007) has produced the revised version of this recommendation which added a new method for the conversion of rainfall rate statistics from 10, 20, and 30 minutes integration time to 1-minute integration time. The 1-minute integration time rain rate has been the recommended time rain rate for the calculation of long-term statistics of rain-induced attenuation (Crane, 2003; ITU-R 530-12, 2007). This is because rainfall rate measured with high-resolution rain gauge, 1-minute or 2-minute resolution resolves the small but significant rain rate, which is needed for the modeling of rain-induced attenuation values. Gauges with longer averaging times will miss the peak-rain-rate values. Therefore, for the prediction of rain attenuation on terrestrial links, a 1-minute accumulation or averaging time is a reasonable compromise.

2.2.6.1 Effect of Integration Time

As a result of the rapidly varying nature of rainfall at a given point, the cumulative rainfall rate distribution measured is dependent on the sampling time of the rain gauge. Since in radio wave prediction techniques, an integration time of one minute is used, Segal has defined a conversion factor, p_T (P) for converting data obtained with a gauge having an integration time of r minutes to equivalent one-minute statistics, as follows (Segal, 1986):

$$p_{r(P)=R_1(P)/R_\tau(P)} \quad (2.1)$$

Where$R_1$and $R_\tau$are the rainfall rate exceeded, with equal probability P, for the two integration times. The factor p_τ (P) is also given by the power law (Segal, 1986):

$$p_t(P) = a - p^b \quad (2.2)$$

over the range 0.001% <P <0 .03%, with a and b being constants that depend on the climatic zone. Watson et al, (1981) considered the conversion factors C_R and $C_e$for rain gauge integration times in the range of 10s to 60 min, given by Segal, (1986);

$$C_e(R) = {}^{e_\tau}/_{e_T} \quad (2.3)$$

$$C_R(t) = {}^{R_\tau}/_{R_T} \quad (2.4)$$

Where $C_e$refers to the ratio of the exceedance (with the same probability P) for a given rain rate R measured using gauges with integration times T and τ; C_R (t) refers to the ratio of rain rates exceeded for a given percentage of time t as measured by rain gauges with integration times T and r. Here, C_R(t) depends on the percentage of time considered (Watson et al 1981). The conversion factors C_R and Ceobtained at Ile-Ife in Nigeria for the measurement madeby Ajayi,between September 1979 to December 1981 using the rainfall rate data obtained from a fast response rain gauge with an integration time of 10 seconds were based on Watson's method (Watson et al 1981). It has also been found that a power law relationship exists between the equiprobable rainfall rates of two integration times.

The power law relationship is given by (Flavin, 1981):

$$R_\tau = aR_T^b \quad (2.5)$$

Where R is the rain rate, τ is the integration time at which the rain rate is required, and T the integration time at which the rain rate is available. (Flavin 1981) also sought a direct and universal expression between 1-minute and 5-minute rainfall rates by examining the cumulative distributions for four locations in Europe, four in North America and five in Australia. From a scatter plot of resulting data points a simple power-law fit was produced giving:

$$R_1 = uR_5^v \tag{2.6}$$

Where $R_1$and$R_5$are the 1-minute and 5-minute rainfall rates exceeded with equal probability, u and v are the regression coefficients (Segal, 1986). The results obtained between 1-minute and 5-minute and between 1-minute and 6-minute integration times were compared and the following relationships were established (Ajayi et al, 1999):

$$R_1 = 0.991R_5^{1.098} \tag{2.7}$$

$$R_1 = 0.991R_6^{1.054} \tag{2.8}$$

Where R_1 is the 1-minute rain rate, $R_5$is the equiprobable 5-minute rain rate value, and $R_6$is the equiprobable 6-minute value. The coefficient a may not be very dependent on climate, while the dependence of b on climate may require further investigation (Ofoche et al 1983).The rain rate data of equipropable at different integration time 1 minute and 60 minutes in Durban are compared by using equations (2.1) and (2.2) (Ofoche et al 1983)

$$\log\left[\frac{R_{imin}}{R_{60min}}\right] = \log(a) + b\log(p) \tag{2.9}$$

Where y = Log (R_{1min}/R_{60min}), m = b, x = Log (p) and c = Log (a)

This is a straight-line equation

$$y = mx + c \quad (2.10)$$

This power law relationship was used to determine the coefficientsa and b with respect to P, the percentage of time for which rain rate is exceeded. Therefore, the conversion factor obtained was used on the Segal power law relationship in equation (2.1) as (Ajayi et al, 1999)

$$R_{1min} = 9.228R_{60min}^{0.8207} \quad (2.11)$$

This has clearly shown a simple power law relationship for the determination of rain rate at the recommended 1-min integration time, $R_{0.01\%}$.

2.2.6.2 Specific Rain Attenuation

The specific rain attenuation (Y) has been found to be empirically related to the rainfall rate through a power law equation given by Moupfouma(2009);

$$Y\ (dB/km) = kR^{\alpha} \quad (2.12)$$

Where the power law parameters k and α are functions of frequency, rain temperature and polarization of the waves, and R is the rain rate (mm/h) (Olsen and Ajayi, 1999).

The ITU-R 838-3 (2007) determined the power law values for k and as a function of frequency in the range of 1 to 1000 GHz (See Appendix 2A); these were developed from curve fitting of the scattering calculations. The values of k and α have been tested to be reasonably accurate for the prediction of specific rain attenuation for frequencies up to

55GHz (Zhang et al., 1999) because beyond this frequency value, the effect of change in soil profile is becoming insignificant. To find the values of the power law parameters k and $\alpha$for both horizontal and vertical polarization for frequency f which lies in between discrete frequencies in (ITU-R 838-3, 2005), logarithmic interpolations are used for f and k, and linear interpolation for α . If k_1, k_2, α_1, and α_2 are the values at frequencies f_1 and f_2 to be interpolated in order to have the power law parameters values at frequency f, then (ITU-R 838-3 (2007);

$$k(f) = \log^{-1}\left\{\log\frac{k_2}{k_1} X\left[\frac{\log(f/f_1)}{\log(f_2/f_1)}\right] + \log k_1\right\} \quad (2.13)$$

$$\propto (f) = \left\{[\propto_1 - \propto_2] X\left[\frac{\log(f/f_1)}{\log(f_2/f_1)}\right] + \propto_1\right\} \quad (2.14)$$

Where k and α are ITU-R Power-Law parameters in equation 2.12, f is a frequency which falls between two discrete frequencies f_1 and f_2 with known parameters k_1, α_1 and k_2, α_2 respectively.

2.2.7 Review of Existing Rain Attenuation Models

A numbers of rain-induced attenuation models exist for different terrains. The key ones are reviewed as follows:

2.2.7.1 ITU-R Terrestrial Rain Attenuation Model

The ITU-R (ITU-R 530-12, 2007) also gives a step-by-step technique for estimating long-term statistics of rain attenuation on terrestrial line-of-sight systems. The steps are as follows:

Step 1: Obtain the rain rate R0.01exceeded for 0.01% of the time with an integration time of 1-minute.

Step 2: Compute the specific attenuation, Y (dB/km) for the rainfall rate at the frequency and polarization of the transmission. ITU-R P.838 provides a method for achieving this using the power-law relationship stated in equation (2.12). Having obtained the specific attenuation corresponding to the reference rainfall rate, the path attenuation needs to be estimated. At this point, it is necessary to recognize that, because of the spatial inhomogeneity present in rain, it is unlikely that a point rainfall rate will extend uniformly over the length of the transmission path, unless this is very short (Hall, 1981; Olsen et al, 1978).The longer the path, the less likely it is that rain will extend uniformly over the full length of the path; hence therefore an effective path length $d_{eff}$is introduced to incorporate this effect (Hall, 1981). This leads to the next step

Step 3: Compute the effective path length, d_{eff} of the link by multiplying the actual path length d of the link by a distance factor r.

$$d_{eff} = rd \tag{2.15}$$

An estimate of this factor is given by: (Olsen, 1999)

$$r = \frac{1}{1+d/d_0} \tag{2.16}$$

where quantity do is a rainfall-rate-dependent factor introduced to reflect the fact that the greater the intensity of rainfall in a storm, the smaller the physical dimensions of the storm. It is given by (Hall, 1981; ITU-R 530, 2007)

$$d_0 = 35\exp(-0.015)R_{0.01\%} \quad (2.17)$$

For $R_{0.01\%} \leq$ 100 mm/h. When $R_{0.01\%} >$ 100 mm/h, 100 mm/h is use in place of $R_{0.01\%}$, as this limits the effects of the reduction factor with increasing rainfall rate (Forknall et al., 2008). Then, finally, the path attenuation exceeded for 0.01% of time is obtained from:

$$A_{0.01\%} = Y_{R0.01\%}d_{eff} = Y_{R0.01\%}rd \quad (2.18)$$

If attenuation statistics are required for other time percentages, for radio links located in latitudes equal to or greater than 30^o North or South, it can be obtained from: (ITU-R 838, 2005)

$$A_p = A_{0.01\%} \text{ x } 0.12p^{-(0.546+0.043\log 10p)} \quad (2.19)$$

And for radio links located in latitude below 30^o North or South, the attenuation exceeded for other time percentages is given as: (ITU-R 838, 2005)

$$A_p = A_{0.01\%} \text{ x } 0.07p^{-(0.855 + 0.139\log 10p)} \quad (2.20)$$

2.2.7.2 Moupfouma Rain Attenuation Model

The Moupfouma rain attenuation model for terrestrial link is grouped under the African attenuation scenario because of the extension of the experimental data utilized in formulating the model to Africa This rain induced attenuation model proposed by Moupfouma in 2009 for rain induced attenuation prediction also employed the power law empirical relationship proposed by (Olsen et al. 1978). The model is based on rain rate exceeded for 0.01% of the time, $R_{0.01}$ (mm/h). This is because it has been established that rain rate data at $R_{0.01}$ and measured with a 1-minute integration time is less variable and

more accurate than the rain rates with highest or lowest time percentages (Moupfouma, 2009). Therefore, provided the rain rate $R_{0.01}$ (mm/h) exceeded for 0.01% of the time is available (may be locally obtained or from the ITU-R data base (ITU-R 838, 2007), the specific rain attenuation on the microwave link can be given as

$$\Upsilon_{R0.01\%} = kR^{\propto}_{0.01\%} \quad (2.21)$$

Where k and $\alpha$are parameters governed by radio link operating frequency and polarization.

During rain events, convective rain cells are often alternated with strati-form rain cells and this leads to variation of the rain cell height (Matricciani and Pawlina-Bonati, 2000). This non-uniformity of rain structure on radio propagation paths leads to the use of equivalent propagation path length, L_{eq}on which the rain structure is assumed to be uniform, rather than the actual path length (Moupfouma, 2009). Therefore, the attenuation exceeded at 0.01% of the time $A_{0.01}$ along a terrestrial line-of-sight link is given as:

$$\Upsilon_{R0.01\%} = kR^{\propto}_{0.01\%} x L_{eq} \quad (2.22)$$

To determine the equivalent path length L_e an adjustment factor δthat accommodates the effect of the non-uniformity of rain along the radio paths is defined as: (Moupfouma, 2009)

$$L_{eq} = \delta x L \quad (2.23)$$

Knowing the rain rate exceeded at 0.01% of the time, the adjustment factor δ is given as

$$:\delta\left(R_{0.01,}L\right) = \exp\left[\frac{-R_{0.01}}{1+\zeta(L)XR_{0.01}}\right] \quad (2.24)$$

Substituting equation 2.23 into 2.22 the equivalent path length, L_{eq} becomes:

$$L_{eq}\left(R_{0.01,}L\right) = L \text{ x } \exp\left[\frac{-R_{0.01}}{1+\zeta(L)XR_{0.01}}\right] \quad (2.25)$$

The equivalent path length of equation (2.25) is dependent on two main parameters namely: the actual path length of the terrestrial link, and the rain rate observed for 0.01% of the time on the radio link. From equation (2.23), the parameter ζL when $R_{0.01} \Rightarrow +0$, is

$$L_{eq}\left(R_{0.01,}L\right) \approx L \quad (2.26)$$

which means when it stops raining on terrestrial radio link, the equivalent path length equals the actual terrestrial radio link path. On the other hand, when $R_{0.01} \Rightarrow +\infty$, then,

$$L_{eq}\left(R_{0.01,}L\right) = L \text{ x } \exp\left(1/\zeta\right)\begin{cases} > Lwhen\zeta(L) < 0 \\ or \\ \leq Lwhen\zeta(L) > 0 \end{cases} \quad (2.27)$$

In equation 2.25, ζ(L) < 0 parameter governs very high rain rates (convective rains), that may cover the entire terrestrial actual path length and over, and ζ(L) > 0 governs convective rains that may just cover less than the actual path length of the terrestrial link (Moupfouma, 2009). The parameter ζ(L) is determined by the magnitudes of the actual terrestrial path lengths of about 34 terrestrial radio links in Africa, Europe, Japan, and United States. Therefore, for terrestrial radio link of propagation length L, such that L ≤ 7 km, then,

$\zeta(L) = -100$ (2.28)

And for terrestrial path longer than 7 km, L > 7 km, then,

$$\zeta(L) = \left[\frac{44.2}{L}\right]^{0.78} \quad (2.29)$$

Finally, rain-induced attenuation for terrestrial line-of-sight link can be predicted with the following expressions (Moupfouma, 2009):

$$\gamma_{0.01} = kR_{0.01}^{\alpha} \text{ x } L \text{ x } \exp\left[\frac{-R_{0.01}}{1+\zeta(L)XR_{0.01}}\right] \quad \text{with} \quad \zeta(L) = -100 \quad (2.30)$$

For any terrestrial link of length L ≤7 km, and,(Moupfouma, 2009)

$$\gamma_{0.01} = kR_{0.01}^{\alpha} \text{ x } L \text{ x } \exp\left[\frac{-R_{0.01}}{1+\zeta(L)XR_{0.01}}\right] \text{with} \quad \zeta(L) = \left[\frac{44.2}{L}\right]^{0.78} \quad (2.31)$$

Whenever propagation path length L >7 km.

This model predicts attenuation governed by a rain rate at a given percentage of time for line-of sight super high frequencies (SHF) and extremely high frequencies (EHF) radio communication links (Moupfouma, 2009)

2.2.7.3 Olsen Rain Attenuation Model

Olsen(1978) found the specific rain attenuation to be related to rain rate through a power-law relation, given as $\gamma = kR^{\alpha}$. This empirical power law relation between the specific attenuation$\gamma$and the rain rate Ris often used in the calculation of rain attenuation statistics because of its simplicity. However, the values of the frequency dependent parameters kand $\alpha$are availableonly for limited number of frequencies. Furthermore, these values

were obtained experimentallyand may contain errors due to limitations in the experimental techniques employed.Olsen (1978) presented a more general theoretical relation between γand Rand confirmedthat the approximation is a good one except in the low frequency and optical limits. In their work,values for kand αare presented for frequency range from 1 to 1000 GHz. These values weredetermined by applying the logarithmic regression to Mie scattering calculations. The power lawcoefficients kand α, cannot be easily represented over several frequency ranges, therefore, fourpower law relationships for both kand α, each valid over a narrow frequency segment, wereestablished for entire frequency range from 1 to 1000 GHz. The four power law relationship forthe values of kandα are given by Olsen (1978) as:

$$k = 6.39 \times 10^{-5} (f)^{2.03} \quad \text{for } f < 2.9\text{GHz}$$

$$k = 4.21 \times 10^{-5} (f)^{2.42} \quad \text{for } 2.9\text{GHz} \leq f \leq 54\text{GHz} \qquad (2.32)$$

$$k = 4.09 \times 10^{-2} (f)^{0.699} \quad \text{for } 54\text{GHz} \leq f \leq 180\text{GHz}$$

$$k = 3.38(f)^{-0.15} \quad \text{for } f > 18\text{GHz}$$

and

$$\alpha = 0.851(f)^{0.158} \quad \text{for } f < 8.5\text{GHz}$$

$$\alpha = 1.41(f)^{-0.0779} \quad \text{for } 8.5 \leq f \leq 25\text{GHz} \qquad (2.33)$$

$$\alpha = 2.63(f)^{-0.272} \quad \text{for } 25\text{GHz} \leq f \leq 164\text{GHz}$$

$$\alpha = 0.618(f)^{0.0126} \quad \text{for } f > 164\text{GHz}$$

where f is frequency in GHz. The power law relationship was adopted by the ITU-R for the calculation of rain attenuation (Olsen et al, 1978)

2.2.7.4 Global Crane Attenuation Model

Rain is characteristically inhomogeneous in the horizontal plane, and a statistical model isrequired to provide an estimate of the effect of the homogeneity on the estimation of attenuation (Crane, 2003). The attenuation model proposed by Crane was based on the kR^{α}rainattenuation model, for attenuation on a horizontal or terrestrial (or path-integrated) link. This issummarized below (Crane, 2003)

$A_{\tau}(R\ D) = kR^{\alpha}\left(\frac{e^{\gamma\delta(R)}-1}{y} + \frac{e^{zD}-e^{\gamma\delta(R)}}{z}e^{\alpha\beta}\right)$ δ® < D < 22.5km (2.34)

$A_T\ (R\ D) == kR^{\alpha}(\frac{e^{\gamma\delta(R)}-1}{y})$ 0 < D < δ®km (2.35)

Where

A_T = horizontal path attenuation (dB)

$kR^{\propto}$ = specific attenuation (dB/km)

and the remaining coefficients are the empirical constants of the piecewise exponential model along the horizontal path length and is represented as:

B = ln(D) = 0.83-0.17ln® (2.36)

C = 0.026-0.03ln® (2.37)

δ®= 3.8-0.6l® (2.38)

$u=\frac{B}{\delta®} + C$ (2.39)

y = αu (2.40)

z = αc (2.41)

For path longer than 22.5km, the attenuation is calculated for 22.5km path, and the resulting attenuation is multiplied by afactor of D/22.5km. This model provides a

prediction of the attenuation or path integrated rain rate given the equiprobable value of rain rate (crane, 2003)

2.2.8 Review of Similar Works

The rainfall characteristics are geographically based due to varying climatic conditions around the world. This has made rain attenuation studies in different regions pertinent as against ITU-R group categorization. A numbers of rain-induced attenuation researches carried out before supported these assertions. The key ones reviewed are as follows:

Agunlejikaet al,(2009) studied the tropospheric Scintillation prediction for some selected cities (Calabar, Enugu, Kebbi, Abuja, Sokoto and Onisha) in Nigeria Tropical Climate. In each chosen cities 12.255GHz and 11.5GHz frequencies were used at 40.1^{o} and 30.73^{o} elevation angle. The prediction based the Scintillation effect on the ITU-R model.It was observed that the Scintillation effect is higher in the coastal site of Calabar and lower in SokotowithRMS amplitude Scintillation value of 0.2dB and 0.07dB respectively and it varies inversely with the elevation angle. The research concluded that scintillation is seasonal. Scintillation intensity strongly depends on $N_{wet}$and is inversely proportional to the elevation angle and directly proportional to the frequency of propagation.The research is merely investigative of the scintillation as a known impairment factor in microwave propagation at frequencies above 10GHz.

Oluwafemi et al, (2009) investigated the effect of rainfall on horizontally polarized radio waves for fixed satellite service at Ku, Ka and V-bands using the Nigeria communication satellite one (NIGCOMSAT-1) in 37 stations in Nigeria. The research focused on 99-99.99% time availability. The result obtained at Ku band downlink shows that 99.99%

was possible in all the 37 stations. At Ka band only 99.9% is practicable in all the stations. At V band downlink 99.99% availability was not possible in all the stations but 99.9%availability was only practicable in the North-west (NW) and North-East(NE) regions, where the attenuation was between 14and 17.9db. The research failed to obtain the rain rate integration at 0.01% ($R_{0.01\%}$) of time, which is fundamental to the probabilities of service availability using ITU-R model.

Omotosho et al, (2009) derived one-minute rain rate distribution in Nigeria from Tropical Rain Measuring Mission (TRMM) satellite data. The results of the rain accumulations from TRMM satellite (1998-2006) were compared with the data collected from 14- ground stations of Nigeria Meteorological Agency (NIMET). The ITU-R recommended 1-minute rainfall ratewas computed using the method developed by Chieko and Yoshio(2002)in which regional climatic parameters such as the thunder storm ratio β were taken into account. It was discovered that the thunderstorm ratio was an important parameter in rain rate estimation. In general, the study showed that the tropical rain measuring mission (TRMM) data closely matches rain gauge data collected from the ground stations in the South-West(SW), South-East (SE), Middle Belt(MB) and North-East (NE) regions of Nigeria. The ITU-R, SG3, digital maps was at variance with the result obtained in all region of Nigeria but the work of Ajayi and Ezekpo(1998) agrees with the present study forSouth-East (SE), South-South (SS), North-West(NW) and North-East(NE) region. This research work was inconclusive for failure to develop rainfall categorization for the different region of Nigeria with 1-minute rain rate result obtained.

Islam et al, (2009)made prediction of fade margins for 15, 23, 26 and 38 GHz frequency bands based on 1-minute rain rate measurements taken over a period of four (4) years at University of Technology Malaysia (UTM) Skudai using the links specifications. The fade margin for all the terrestrial links were measured based on the rain attenuation data collected at different hop lengths. The result obtained was used as feasibility study to design an outage-free wireless broadband radio link and it reviewed the specifications for Broadband Fixed Wireless Access BFWA) system such as Local Multipoint Distribution Service (LMDS) and IEEE 802.16 in tropical region. The research work did not show result validation using any of the known standard models.

Abdullah et al, (2010) determined the coefficients of k and α of power law relationship for the computation of specific rain induced attenuation using three years rain gauge and beckon data taken from University of Science Malaysia, (USM) NibongTebal. The research showed a year-to-year variation in theITU-R coefficients of k and α for the region withthe measured data. It was concluded that the ITU-R recommendation for regression coefficient of rain specific attenuation is not suitable for predicting rain attenuation in Malaysia. However, the research should have considered more experimental data from other location in Malaysia because regional climatic change and use mean values of data obtained to draw inference.

Das et al, (2010) measured raindrop size distribution with distrometer at five different locations in the Indian tropical region. Lognormal distribution model was used to model rain induced attenuation for the frequency range 10-1000GHz. Different attenuation characteristics were observed for different regions due to the dependency of drop-size

distribution values derived.At frequencies below 30GHz, the ITU-R model matches with the drop-size distribution generated values but differ significantly at higher frequencies. This suggests that more measurement is required for modeling rain induced attenuation at EHF bands in the tropical region. The research assumed lognormal distribution model as ideal for drop-size distribution estimation in the tropical region. A better inference would have been drawn if the measured data were used on other models like Laws and Parson's, Marshal and Palmer, Wiebull, Gama and modified Gama distribution models for comparison

Lam, (2010), provided additional information about the performance of the SC EXCELL model, specifically when applied to rain attenuation in equatorial regions. The model generated a long-term rain attenuation cumulative distribution function (CDF) that separately accounts for stratiform and convective precipitation. The most assessment in estimating attenuation CDFs due to rain are carried out against experimental data for three particular South–East Asia regions, namely Kuala Lumpur, Singapore and Thailand. The over estimation outcomes of the model suggest that to correctly predict rain induced attenuation on satellite communication links, the concurrency between rain induced attenuation and rain intensity measurement should be taken into account. Application of this research work to tropical region of Africa would require more investigation because rainfall in most of the regions is a combination of both stratiform and convective rain.

Odedina, (2010) made a statistical analysis of rain fade data and proposed an empirical rain attenuation model for South Africa locations. The research was targeted at the

theoretical rain induced attenuation prediction models based on the assumption that the shapes of raindrops were spherical. The results obtained showed that it was not the raindrop shapes that determine the attenuation due to rain but rather the rain rate content in the drops and the drop size distribution. The comparison made with the ITU-R standard provided update for the various percentages of link availability in South Africa. The research work utilized the rain rate integration concept at 0.01% ($R_{0.01\%}$) proposed by Ajayi et al, (1999) for South Africa climate. It however, used the mie scattering coefficient by the ITU-R for parameters k and α. The effects of these two parameters were more important factors in the rain-induced attenuation and should have been investigated for the region.

Folaponmile et al, (2011), proposed an empirical model for the prediction of Mobile Radio Cellular signal attenuation in harmattan weather. The research used measure Received Signal Level(RSL) at 1800MHz for 18months. The dust densities and the measured RSL were used for the model development. The result proposed a correction factor of 18.8dB to Link budget. The developed linear model was validated with the measurement. The research failed to make comparison with any standard and accepted model for validation.

Khairayu et al, (2011) studied rain induced attenuation for V-band satellite communication in tropical region. Attenuation due to rain at 38GHz was measured for a period of 20-months in Malaysia and presented as monthly diurnal and annual statistics of rain attenuation. The results suggest an overview of how 38GHz satellite Earth link might propagate because a severe attenuation of up to 38dB for 99.99% availability in a

year was observed. But all the comparison made with some of the existing model including the ITU-R model exhibit marginal deviation at 0.1-0.001% time exceedance. Hence there is need for further investigations to accurately predict the rain attenuation at V-band frequencies.

Parshotam et al, (2011)estimated path length reduction factor by using one-year rain-induced attenuation statistics over a line-of-Sight (LOS) link operating at 28.75GHz in Amristar (INDIA). A new concept of path length reduction factor, which account for the inhomogeneous nature of rain droplets, along the path length of the microwave signal was proposed. A marginal difference in the path length reduction factor when compared to the ITU-R prediction was observed as the significant cause of ITU-R prediction error for the region. The research work focused only on the effective path length in the estimation of rain-induced attenuation. There is need to establish a relationship for the rainfall effective slant height with the new path length concept for satellite communication design for the region.

Alonge et al, (2012) undertook seasonal analysis and prediction of rainfall effects in Eastern South Africa at microwave frequencies. The seasonal approach was used to estimate for the effect of spacial rainfall induced attenuation in Durban South Africa using two (2) years rainfall data obtained from RD-80 (J-W) distrometer. Consequently, rainfall drop-size distribution models were developed for the control site at different season. The probability analysis indicated that the lognormal distribution best fits the summer and autumn season with RMS Error of 30% and 26% respectively; gamma distribution fits winter season with RMS Error of 16%. The result obtained from the rain

rate and the rainfall drop-size distributions were combined to estimate for specific rain induced attenuation using Mie scattering techniques between 2GHz and 100GHz. It was concluded that the predicted specific attenuation coefficients for all season rainfall rates at control site were lower, when compared to those from ITU-R models. The inference drawn suggesteda review of the ITU-R prediction for a more efficient link budget.

Isikwue et al, (2013) Presented attenuation of Radio Communication Links inMarkurdi, Nigeria using rain fall rate analysis at 0.01% of time from five-minute rain data measured by the Nigerian Environmental and climate observing program (NECOP) in the University. They employed the Chebil, Moupfouma and ITU-R prediction models to arrive at an average of 112mm/h rain rate. The study concluded with the adoption of Chebil rain rate model for a better prediction. However, the height of the Nigerian Environmental and climate observing program (NECOP) used for the rain measurement is too close to the ground and could introduce errors in the measurement.

Seker et al, (2013)performed the simulation of attenuation in mobile communication due to atmospheric events like snow and rain using discrete propagation model. In the research work spherical raindrop and oblate spheroid raindrop were considered. Oblate spheroid raindrop modeling produced results that were more compatible with ITU-R result, especially at frequencies higher than 50GHz. At lower frequencies both raindrop shapes modeling results were not compatible with the ITU-R result.The study concluded that snow attenuation was higher than rain attenuation because of the particle size. In all simulations, frequencies of GSM communication of 900MHz, 1800MHz and 2270MHz were used. The research work assumed only uniform distributions of the particles.

Exponential distribution method should have been investigated too for comparison because of the snowflakes varied densities.

2.2.9 Summary of Chapter Two

All the researches reviewed for this work were based on the basic fundamental concept and direct comparison of results with some of the world acceptable existing models that are currently being put to contest because of some perceived errors. These errors are due to the different features and climatic conditions associated with regions around the world, which directly influence the rain in a particular environment. It's therefore evident that the globalization of rainfall and structures by ITU-R to vast group of regions motivate the different researches carried out. Most of the models developed and reviewed in this dissertation were based on:

i. The cumulative distribution of rain rate at a point (Moupfouma, 2009).

ii. The concept of equivalent path averaged or integrated rain rate along the propagation path length, (Crane, 2003).

iii. The concept of effective path length or effective rainfall rate (Moupfouma, 2009), (ITU-R 530-12, 2007)

iv. That the raindrops are assumed to be spherical water droplets which caused signal attenuation. The attenuation is due to both energy absorption losses in the raindrops as well as scattered energy by water droplets from the incident radio waves, (Matzler, 2002b)

v. The assumption that each drop's contributions are independent of the other drops, and the contributions of the drops are additive, (Matzler, 2002b),

vi. Many others based it on the theoretical microphysical structure of the rain (Olsen et al, 1978).

Generally, allthese based on analytical models using the microphysical structures of rain from the different regions where the researches were carried out. In this dissertation however, empirical models were developed for the prediction of rain induced attenuation for the 13GHz and 15GHz microwave frequencies based on direct measurement of received signal levels (RSL) of the links because of the correlation between the extracted rainfall rate and the measured attenuation.

CHAPTER THREE

MATERIALS AND METHOD

3.1 Introduction

Theoretical models which can be used to forecast the rain induced attenuation on microwave communication link at 13GHz and 15GHz frequencies were developed. The rain rate being an independent variable has a direct relationship with the measured rain attenuation given that the polarization of the antenna and the effective path length of the rain remain constant. Linear regression analysis is thus employed as a tool in developing the model using least square method. But the ITU-R terrestrial attenuation model is non-linear (Power-law given by $A_p = aR^b$) andnon-linear models are more difficult to fit than linear models because the coefficients cannot be estimated using simple matrix techniques, instead, an iterative approach is required. Therefore,linear least squares fitting would be applied iteratively to a linearized form of the function until convergence is achieved. The iteration is based on Microsoft Excel software using the Trend-line function as a scatter chart. Any curve fitting function derived from the chart produces adequate proportion of the variability in the data explained by the model over the total variability of the data. This method is adopted because it attempts to measure the degree of correlation which exists between the dependent and independent variables and thereby establishing the independent variable predictive value.The developed models were

evaluated by the tread-line regression coefficient and by using statistical techniques of Chi-Square Test and Root Mean Square Error. The ITU-R terrestrial attenuation model was used for the validation of the developed empirical models.

The model development was a followed up to the data collection, measurement and processing. The data measurement is made possible by the permission of Airtel Network operation office in Kaduna. The measurement conducted covered the two rainy seasons of year 2009 and 2010. NigerianMeteorological Agency (NIMET) provided the rainfall data for the two years. Figure 3.1 below showed the block diagram for the materials and method adopted.

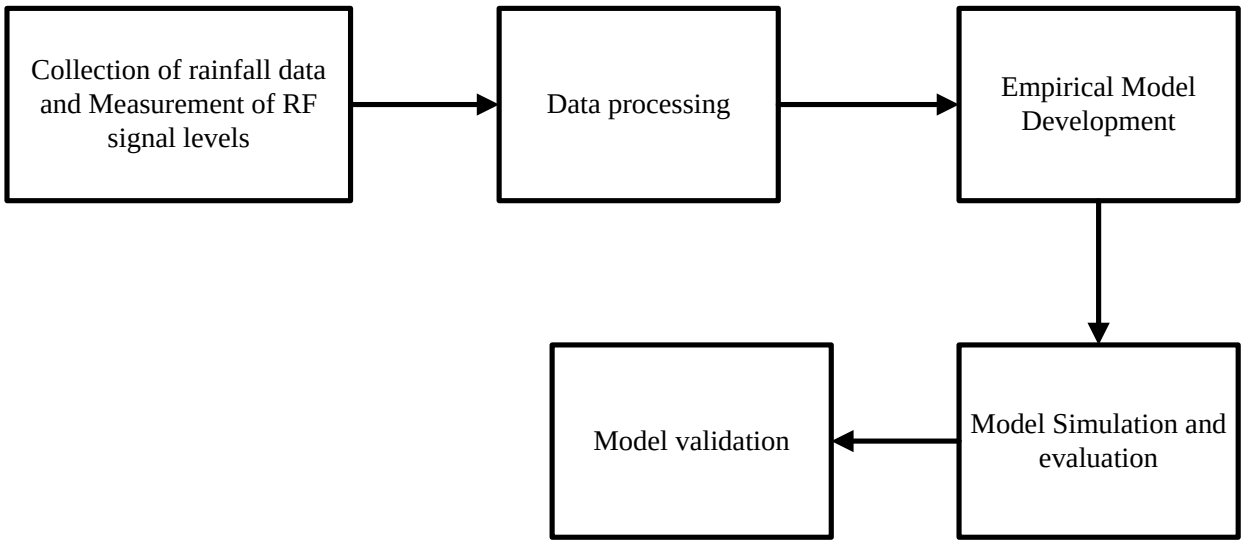

Figure 3.1: Block Diagram for the Materials and Method

3.2 Data Collection and Measurement

The rainfall data was collected from the Nigerian Meteorological Agency (NIMET). The rain data collected was for the 2009 and 2010 rainy season, Appendix 3A. The raw data was processed for the monthly average rain rate used for the model development. Two

years received signal levels (RSL) of the two links (13GHz and 15GHz) were measured at clear sky and during rain fall (Appendix 3B). According to ITU-R (Rec. ITU-R PN.676-1, 1992), clear-sky is taken to be the condition of intrinsic atmospheric attenuation due to gases and water vapour without excess attenuation due to tropospheric precipitation such as rain and snow, (Intelsat, 2006).Airtel GSM Base Station Controller (BSC) links operating at 13GHz and 15GHz were used. The measured RSL were processed for the rain induced attenuation. Other link propagation parameters were obtained from the link document,Appendix 3C. The Network operator made the link document available for this research work.

3.2.1 Measurement Set-up

Figure 3.2: shows the block diagram of the link setup used for the measurement taken for this research work.

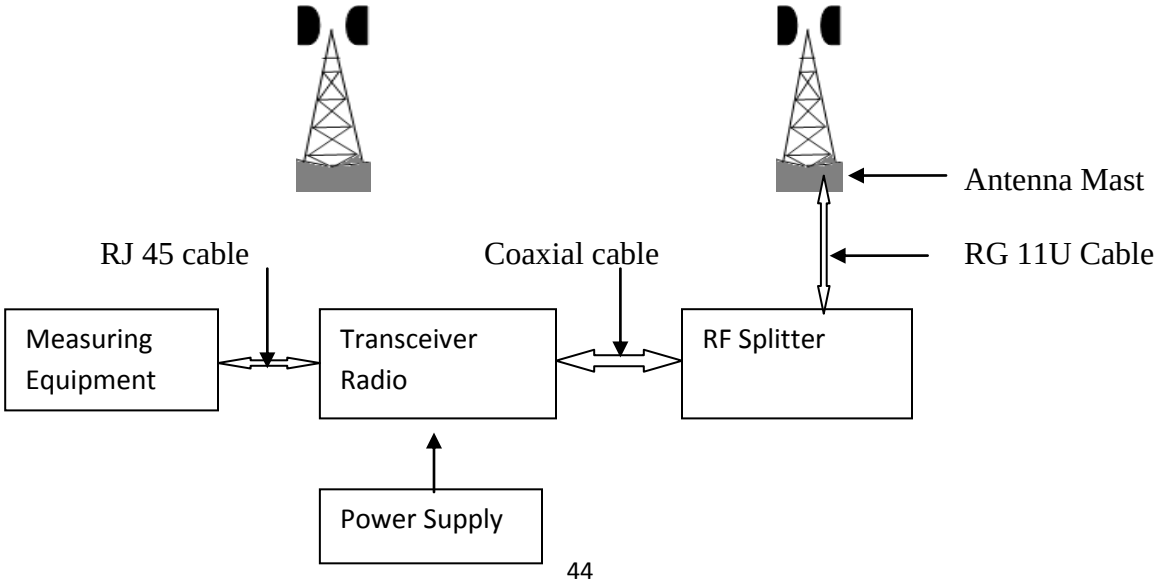

Figure 3.2: Block Diagram of the Measurement set up

The transceiver radio was a HD radio model SRA 4. Theradio provides dedicated high capacity wireless connections from single to multiple 155Mb/s data channels up to a total transport capacity of 622Mb/s. It provides the base station backhaul communication link services in the BSS.

The RF splitter was used in the system for frequency distribution. The splitter was a 1 to 12 configuration type. The 1-end connects to the antenna and 12-end connect to the different transceiver radios transmit (Tx) and receive (Rx) on the program installation equipment (PIE) rack.

The mast carried the Andrew VHLP4 (Valuline High Performance Low Profile) parabolic antenna connected to the transceiver radios through RF Splitter with RG 11U coaxial cable. The set of transceivers were interconnected through an Ethernet switch to the measuring equipment.

The measuring equipment was a branded Dell Power Edge 2800 computer dedicated for the links configuration and performance monitoring. The computer had a window based mini-link craft versions 2.13 Software installed for its operation and direct capturing of the links received signal levels (RSL).

A 20kVA UPS with two 27kVA Perkins generators back-up provided an uninterrupted power supply to the radio system.

3.2.2 Direct Measurement of the Received Signal Levels (RSL)

The received signal levels (RSL) of the two links of 13GHz and 15GHz were captured over a period of two rain seasons in Kaduna. The rainfall season covered a period of seven calendar months (April to October) of 2009 and 2010. The 13GHz measurement snapshots of the received signal levels taken with the aids of the measuring equipment on clear sky and during rainy conditions are shown Plate 3.1 and Plate 3.2

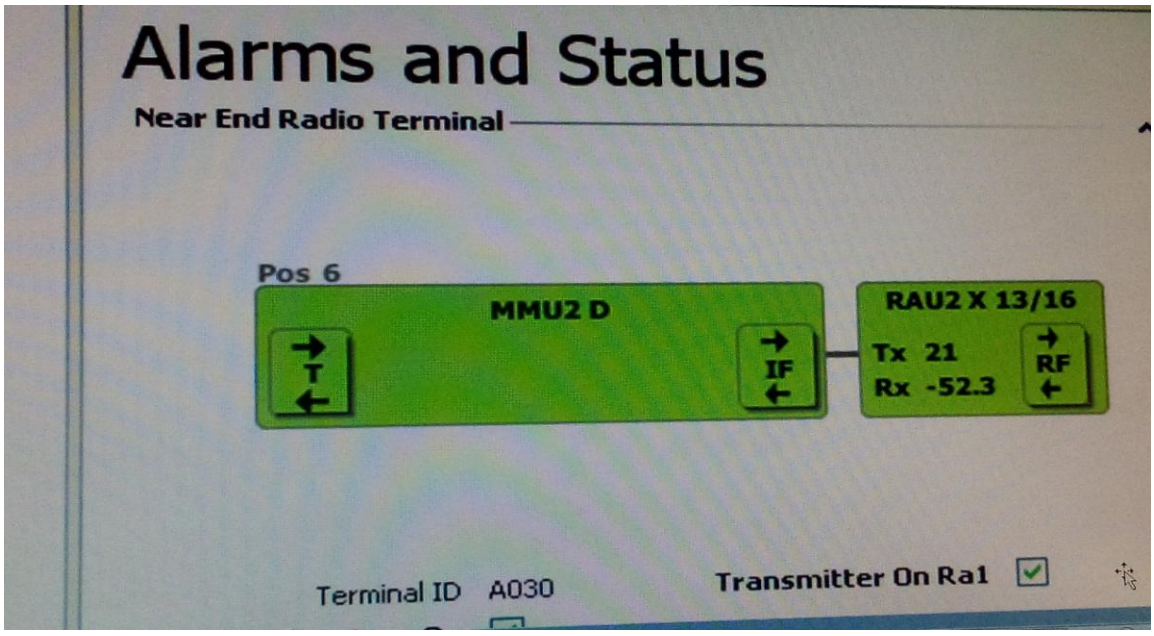

Plate 3.1: 13GHz clear sky RSL

Plate 3.1 showed a captured received signal level of -52.3dBm on clear sky. The signal was from transmitter 21 with terminal ID A030. The same transceiver captured received signal level of -56.1dBm during rain event as shown below in Plate 3.2.

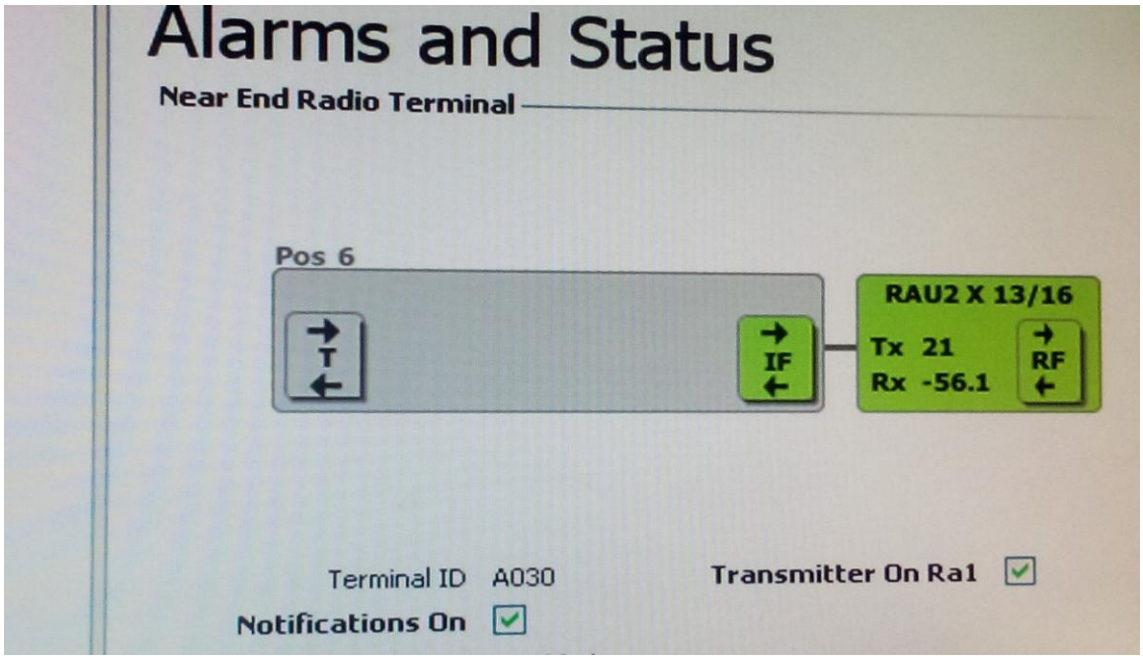

Plate 3.2: 13GHz Rain Condition RSL

The same procedure shown in Plates 3.1 and 3.2 was followed for the 15GHz microwave link. The captured received signal level of the links was used for the links performance analysis and direct estimation of the excess attenuation of the links due to rain drops on the antenna for both the 13GHz and 15GHz microwave link.

3.3 Data Processing

The rain rate used in this research work was extracted from the NIMET rainfall data. The measured link received signal levels (RSL) was processed as the link performance analysis to extract the link fade margin and the monthly average rain induced attenuation.

3.3.1 Analysis of the Extracted Rain Rate

Two years rainfall data was obtained from the Nigeria Metrological Agency (NIMET). The data collected from NIMET covered the absolute rainfall of two rainy seasons, April to October of year 2009 and 2010 (Appendix 3A). The raw rainfall data of amount of rain and the duration of rainfall was used to calculate the average rain rate shown in Table 3.1

Table 3.1: Monthly Mean Rain Rate for Kaduna, 2009 and 2010

MONTHS	RAIN RATE mm/h		
	2009	2010	Mean Rain Rate
APRIL	6.16	18.39	12.33
MAY	14.99	19.13	17.06
JUNE	25.05	36.11	30.58
JULY	17.01	29.85	23.43
AUGUST	45.95	32.24	39.10
SEPTEMBER	19.38	35.22	27.30
OCTOBER	21.86	21.37	21.62

Table 3.1 showed that June and September 2010 had the highest rainfall intensity followed by July and August of the same rainy season. April and May of the year experience same rain fall rate on the average. In June the rain intensity was higher with shorter duration but the duration of rainfall for the August was much longer. Therefore, the impact of the high rainfall on the microwave antenna was more in August and September.In 2009 however, there was moderate rainfall regime except in August when the rain intensity was higher. Then 2009 recorded longer duration of rainfall with 95 rain events but the average rainfall rate is much higher in 2010.

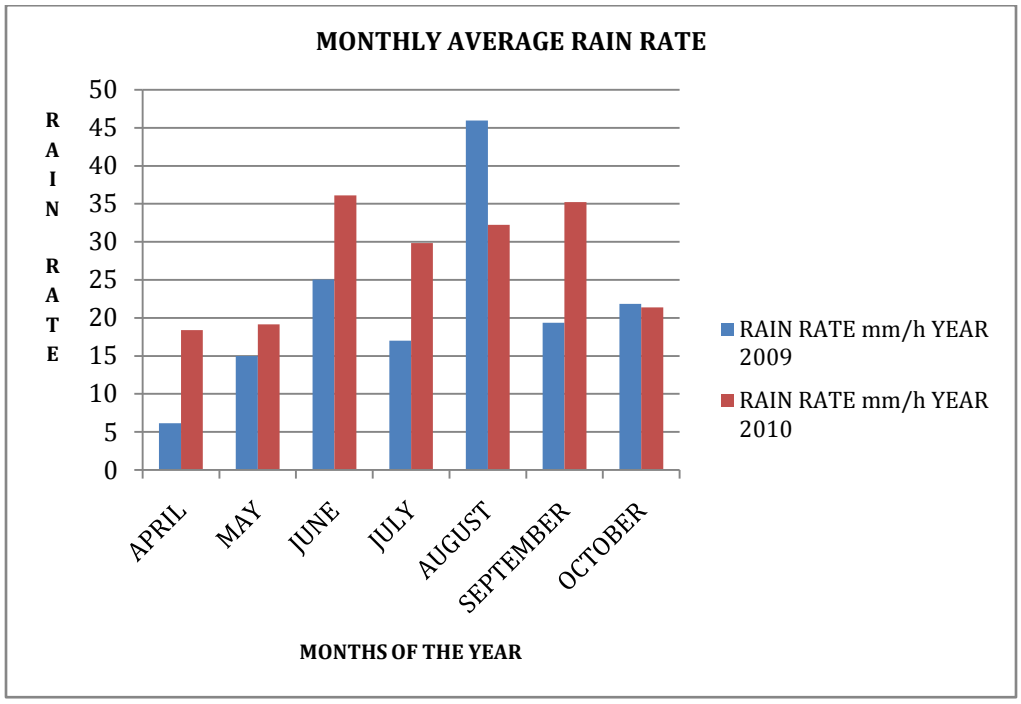

Figure 3.3: Monthly Average Rain Rate for 2009 and 2010 in Kaduna

The measured rain rate showed higher values in 2010 as compared with 2009. But August 2009 has the highest rain events and rain rate value of 45.95mm/h. The year 2009 also had the lowest rain rate in April with 6.16mm/h. Figure 3.3 presents the monthly average rain rate for the two rainy seasons and developed to the year mean values for model development.

3.3.2 Microwave Links Performance Analysis

Generally, the captured received signal level RSL for each of the link was lower in the 2009 rainy season when compared with that of 2010 except for August 2009 when the rainfall was higher as shown below in Figure 3.4 and Figure 3.5.

With the exception of certain rain events, the severity of the signal degradation was tolerable during the rain events of 2009 and 2010 by the two links because there were few cases of the received signal level RSL crossing the threshold. The threshold level for the

links and other link budget consideration was extracted from the link document Appendix 3C as shown in Table 3.2

Table 3.2: Link Design Parameters

Frequency Bands(GHz)	Maximum transmit power in dBm	10^{-6BER} Receive threshold(dBm)	Antenna spec. Both trans & receiver	
			Size (m)	Gain (dB)
13	+14	-73.50	0.6	42.00
15	+10	-73.00	0.6	42.90

The rain events at some instance like August 2009 however gave a different account of the link performance as shown in Figure 3.4 and Figure 3.5.

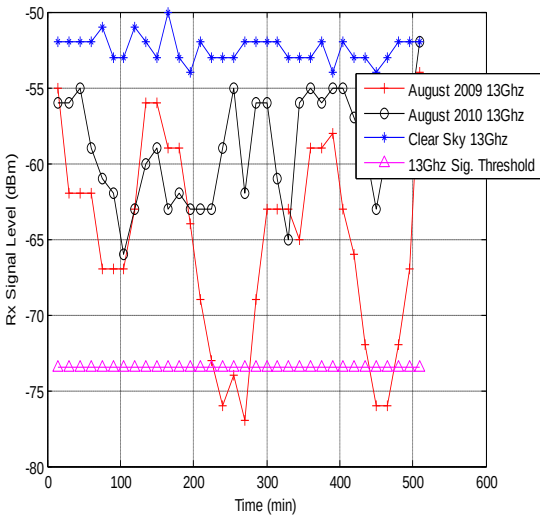

Figure 3.4: 13GHz Link RSL Variation

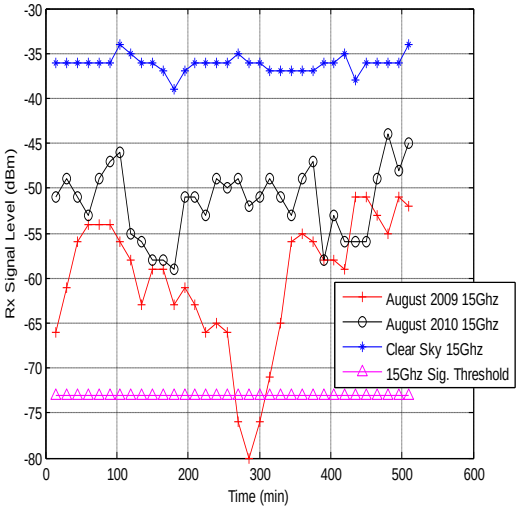

Figure 3.5:15GHz link RSL Variation

The link performance analysis showed clear cases of loss of service thrice by the 13GHz link at certain instant of the rainfall when the RSL crossed the threshold level of -73.5dBm. The RSL of the links at these instances fluctuate between -77dBm and the threshold. In the same month of August 2009, the 15GHz link service was disrupted by rainfall when the RSL of the link goes higher to about -80dBm against the threshold level

of -73dBm. This instance indicated absolute fade margin of -77dBm and -80dBm for the 13GHz and 15GHz microwave links respectively in August 2009.

Statistical evaluation of the captured RSL data was developed to the monthly mean and median(Appendix 3B) and summarized as shown in Table 3.3 and Table 3.4

Table 3.3: Monthly Mean and Median of 13GHz Link faded RSL

YEARS	2010		2009	
Months	Mean RSL (dBm)	Median RSL (dBm)	Mean RSL (dBm)	Median RSL (dBm)
APRIL	-55.80	-56	-54.53	-54
MAY	-58.00	-57	-55.07	-55
JUNE	-63.73	-66	-58.73	-58
JULY	-58.80	-58	-55.13	-55
AUGUST	-59.27	-59	-65.40	-64
SEPTEMBER	-61.20	-59	-61.20	-59
OCTOBER	-58.07	-57	-58.47	-58

Table 3.4: Monthly Mean and Median of 15GHz Link faded RSL

YEARS	2010		2009	
Months	Mean RSL (dBm)	Median RSL (dBm)	Mean RSL (dBm)	Median RSL (dBm)
APRIL	-40.38	-39	-40.25	-40
MAY	-44.20	-43	-41.67	-42
JUNE	-54.33	-51	-50.60	-50
JULY	-51.40	-49	-41.00	-40
AUGUST	-51.53	-52	-60.20	-62
SEPTEMBER	-53.13	-53	-42.53	-42

OCTOBER	-47.00	-46	-50.33	-52

The statistical evaluation showed that the 13GHz microwave link had an average signal fade margin of -65.40dBm against the clear sky value of -52.45dBm during the August 2009 heavy rainfall. The 15GHz link indicated an average fade margin of -60.20dBm against the clear sky mean value of -36.45dBm in the same period. The monthly mean RSL values was adopted and used for the direct estimation of the rain attenuation for each microwave frequency.

3.3.3 Rain Induced Attenuation

The difference between the faded received signal level due to rain drops and the clear sky (None faded) signal level captured from the links was used as the measured rain induced attenuation.

Table 3.5:Measured Rain Attenuation for 13GHz and 15GHz Links in 2009 and 2010

Months	13GHz Measured Attenuation (dB)			15GHz Measured Attenuation (dB)		
	2009	2010	Mean (A_p)	2009	2010	Mean (A_p)
April	2.08	3.35	2.72	3.11	3.93	3.52
May	2.62	5.55	4.09	4.55	7.75	6.15
June	6.28	11.28	8.78	12.95	17.88	15.42
July	2.68	6.35	4.52	6.28	14.95	10.62
August	12.95	6.82	9.89	19.95	15.08	17.52
September	8.75	8.75	8.75	7.95	16.68	12.32
October	6.02	5.62	5.82	11.95	10.55	11.25

The measurement showed a high correlation with the rainfall rate extractedin Table 3.1. Year 2010 generally had more signal attenuation due to rainfall than 2009. However, in

August 2009 the 13GHz link had the highest rain induced attenuation of 12.95dB and a mean value of 9.89dB for the two years. The 15GHz link also had 19.95dB excess rain induced attenuation in August of year 2009 and a mean value of 17.52dB for the two years. The mean measured value of the rain induced attenuation was used as data for the model development.

3.4 Development of the Empirical Model

The least squares method is used in this research modeling because it assumes that the best-fit curve of a given function is the curve that has the minimal sum of the deviations squared for a given set of data. The outcome of event is deterministic unlike stochastic method which is a repeating process whose outcomes follow no describable deterministic pattern but follow a probability distribution, such that the relative probability of the occurrence of each outcome can be approximated or calculated.

This was based on linear regression analysis.Linear model was used to examine the relationship between dependent and the independent variables. After performing an analysis on data, the regression statistics can be used to predict the dependent variable when the independent variable is known. This was normally being represented as:

$$Y = \text{intercept} + (\text{slope}, X) + \text{error} \quad (3.1)$$

Where Y is the dependent variable and X is the independent variable

Even though the ITU-R power-law fits the non-linear least square relationship between the values of the independent and the corresponding conditional dependent mean values, the regression function was linear in the unknown parameters that are estimated from the data. For this reason the regression was considered iterative. Software solution like

MATLAB or Microsoft Excel spreadsheet could be used for finding the best-fitting curves giving a set of points by minimizing the squared error. The Tread-line function of the Excel software is chosen for the modeling because it runs on C++ program without additional codes and easy display of the curve-fitting evaluation with the coefficient of regression R^2. Besides, gradient (slope) and intercept of the linear least squares fit are determined by statistical analysis.

3.4.1 Linear Regression

Nonlinear regression problems can be moved to a linear domain by a suitable transformation of the model formulation.

Considering the ITU-R model

$$A = aR^b \tag{3.2}$$

with parameters *a* and *b*. If we take the logarithm of both sides, this becomes

$$\ln(A) = \ln(a) + b\ln(R) \tag{3.3}$$

This has been clearly transformed to the linear regression equation (3.1)

The goal of regression analysis was to model the expected value of a dependent variable *y* in terms of the value of an independent variable*x*. In simple linear regression, the model use was

$$y = a_0 + a_1 x + \varepsilon, \tag{3.4}$$

Where ε is unobserved random error with mean zero condition on the independent variable *x*. In this model, for each unit increase in the value of *x*, the conditional expectation of *y* increases by a_1 units.

In general, we can model the expected value of *y* as an *n*th degree polynomial, yielding the general polynomial regression model for increased conditional expectation of y.

$$y = a_0 + a_1 x + a_2 x^2 + a_3 x^3 + \cdots + a_n x^n + \varepsilon. \quad (3.5)$$

In this dissertation, the mean rain rate (*x*) in table (3.1) is the independent variable and the mean measured attenuation (*y*) in Table (3.5) is the dependent variable. The Excel Trend-line function chart was used to model for the best curve fitting functions as polynomial and power-law curve fittings. The functions were further evaluated using statistical techniques.

3.4.2 Microsoft Excel Trend-line Function Plots

This is a graph of plotted points that shows the non-linear relationship between two sets of data, example, rain rate and measured attenuation. Thefunction plot for curve fittings using the excel tool gave the best-fit line or curve on a graph for the input data. This tool was chosen because the two sets of data involved had high correlation between the dependent and the control or the independent variables. When the lines of best fit were plotted as shown in Figure 3.6 and Figure 3.7, using the mean measured rain Induced attenuation for each of the link, a careful study indicates a positive correlation. Since a correlation exists, then some sets of equations describing the fit can be generated. From the plots, a set of equations and their regression coefficients that show the measure of accuracy of the model were displayed on the graph.

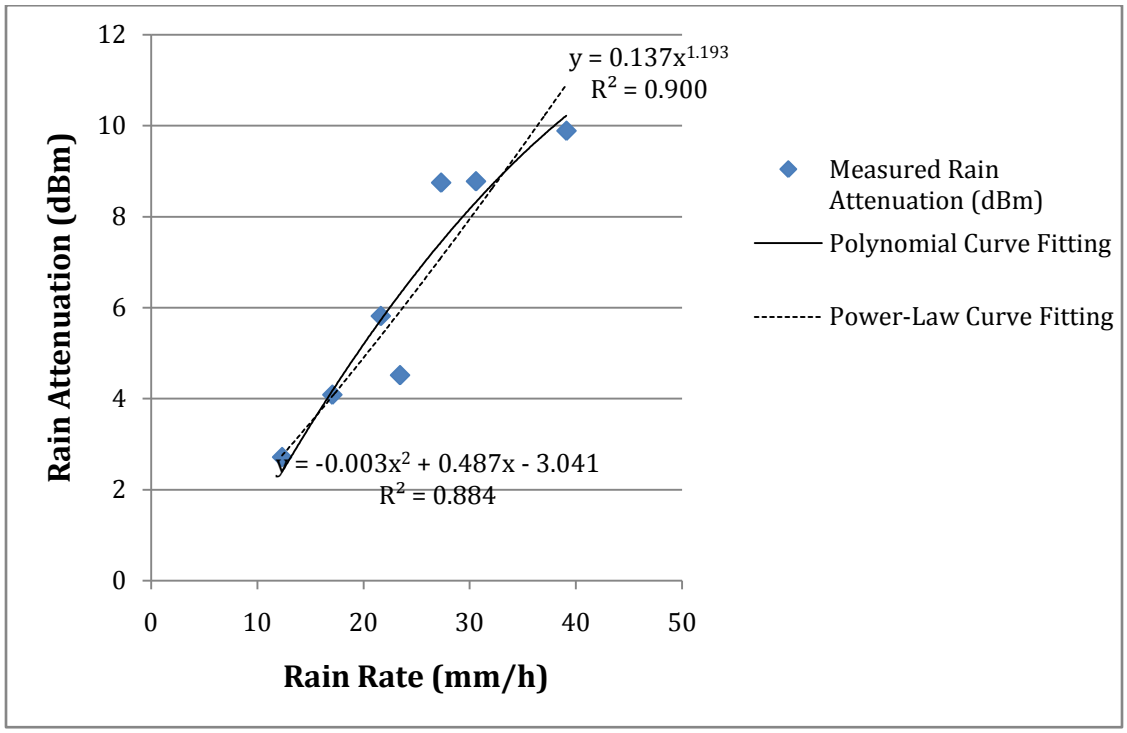

Figure 3.6: Predicted Rain Induced Attenuation Model at 13GHz

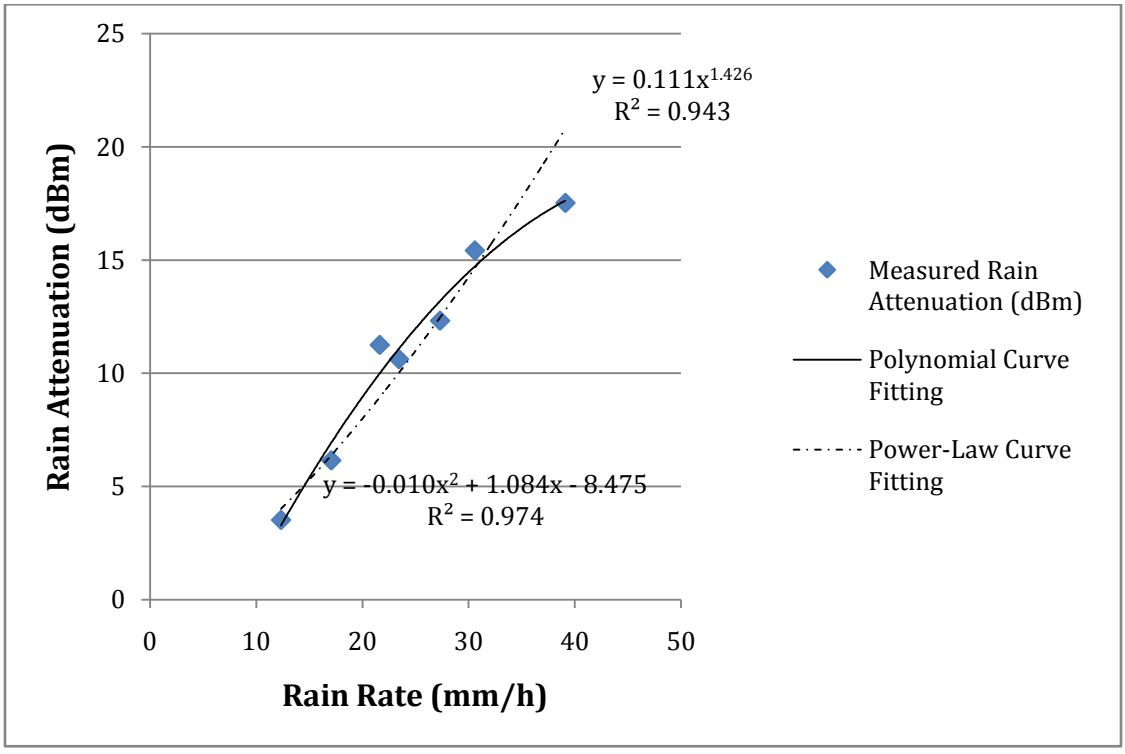

Figure 3.7: Predicted Rain Induced Attenuation Model at 15GHz

3.4.3 Least Square Fitting

Conveniently, these models are all linear from the point of view of estimation, since the regression function is linear in terms of the unknown parameters a_0, a_1, ...α n. Therefore, for the least squares analysis, the computational and inferential problems of polynomial regression can be completely addressed using the techniques of multiple regressions. This is done by treating x, x^2,...x^nas being distinct independent variables in a multiple regression model.

Our concern here was only the polynomial curve fittings because it best described the data point as evaluated using statistical techniques.The slope and intercept of the linear least squares fit from the curve fitting can be computed on the Excel spreadsheet in a step wise ways as follows using the same dependent (y) and the independent (x) mean data.

Calculate the intermediate product of 'xy' and x^2

Calculate the intermediate sum of "Σx, Σx^2, Σ y, Σ xy"

Calculate the Numerator as n(Σ xy) – (Σ x)(Σ y) and (Σ y)(Σ x^2) (Σ x)(Σ xy)

Calculate the Denominator as n(Σ x^2) – (Σ x^2)

Where n is the number of the data points. The slope (m) and the intercept (C)of the regression is given by

$$m = \frac{\mathrm{n}(\square \mathrm{xy}) - (\square \mathrm{x})(\square \mathrm{y})}{\mathrm{n}(\square \mathrm{x2}) - (\square \mathrm{x2})} \tag{3.6}$$

$$C = \frac{(\square \mathrm{y})(\square \mathrm{x2})\,(\square \mathrm{x})(\square \mathrm{xy})}{\mathrm{n}(\square \mathrm{x2}) - (\square \mathrm{x2})} \tag{3.7}$$

However, simulation of the polynomial curve fittings was adopted in this work using MATLAB R2008a to show the possible linear regression of the functions whose slope m,

and intercepts, c could be determined with further statistical analysis of the standard deviation and the means model error.

3.5 Model Evaluation and Simulation

The predicted curve fitting functions were evaluated using the chi-square test and the root mean square error (RMSE) statistical techniques. The chosen polynomial fittings were simulated using signal processing toolbox of MATLAB R2008a.

3.5.1 The Chi-Square Test

The Excel scatter function charts had displayed a number of equations based on the curvefit and the regression coefficients for each of the curve. Therefore the Chi-Square Test was used to further analyze and testeach of the equation to determine the curve that best define the data points.The chi-square statistic is used to determine the error bounds between models and measurements while the RMS percentage error determines the measure of the error (in percentage) between the model and the measurement.These two statistical tools were employed and used on the curves that gave the best description of the mean measuredrain attenuation data points in Figure 3.6 and also the best fits in Figure 3.7

The chi- square statistic is also used to validate the acceptance or rejection of the null hypothesis of a model or relation. According to (Freedman et al. 1978), the chi-square statistic is given as:

$$\mathbf{x^2} = \sum_{\mathbf{i=1}}^{\mathbf{N}} \frac{(\mathbf{x_{mea,i} - x_{pre,j}})^2}{\mathbf{x_{pre,j}}} \qquad (3.8)$$

Where Xmean is the mean measured rain attenuation values of each link, Xpred is the

predicted values from the analytical curves, N is the number of measured or predictedpoints ranging from 1,2...7 in this context.

Table 3.6: Chi-Square Statistics of the Analytical Curves

LINK	Degree of freedom(N-1)	Analytical Curves	Chi-square	Hypothesis at 5% level of Confidence
13GHz	6	Polynomial	0.81	Accepted
		Power-Law	0.75	Accepted
15GHz	6	Polynomial	0.38	Accepted
		Power-Law	1.27	Accepted

In a chi-square statistic problem, the degrees of freedom (N-1) for the number of mean measurements recorded in each year must be determined so that the threshold values for the chi-square test at each level of confidence or significance level can be analyzed.

For this work, the chi-square test was determined at a threshold value of 5% level of confidence. Appendix 3D is the reference Chi-Square distribution table used for the acceptance or otherwise of the hypothesis. The Chi-square test result of Table 3.6showed that the entire curve fitting functions can be reasonably used to predict excess rain induced attenuation values for the links since the test certified all the equations as acceptable analytical models.

3.5.2 Root Mean Square Percentage Error

To further evaluate the model that best predict the mean measured rain attenuation data points for each of the link under observation; the root mean square (RMS) percentage error was used. Table 3.7 showed the RMS percentage error computed for the evaluation of the best curve fitting functions. The root mean square error function was given by

$$\Delta_{rms} = \sqrt{\frac{1}{N}\sum_{i=1}^{N}\left[\frac{100(A_{m,i}-A_{p,j})}{A_{m,j}}\right]^2} \quad (3.9)$$

Where there were Nth data points with A_m and A_p as the measured and the predicted Attenuation for the i^{th} occurrence respectively. Based on the RMS percentage error for the curves, the curve with the lower percentage error was adopted as the best-fit model to predict the rain attenuation for each of the link.The polynomial functions showed appreciable variability and statistical acceptance for the rain induced attenuation observed in Kaduna-Nigeria for the period of two the years, 2009 and 2010 with the lowest root mean square error (RMSE). The root mean square error analysis results in Table 3.7 showed the polynomial functions as the best curve fittings for both the 13GHz and 15GHz measured data.

Table 3.7: Root Mean Square Percentage Error for the Analytical Curves

LINKS	Analytical Curves	RMSE
13GHz	Polynomial	0.86
	Power-Law	0.96
15GHz	Polynomial	0.73
	Power-Law	1.57

These polynomial functions in Table 3.8 below were the developed empirical models described by the measured rain attenuation data points.

Table 3.8: Predicted Empirical Models

LINKS	Predicted Empirical Models
13GHz	$Ap=-0.0038Rp^2+0.4878Rp-3.0414$
15GHz	$Ap= -0.0107Rp^2+1.0848Rp-8.4759$

3.5.3 Simulation of the Developed Model

The predicted empirical models were developed for forecasting rain induced attenuation of the 13GHz and 15GHz microwave frequencies when there are rain drops on the antenna. The method used practically showed the degree of correlation of both the dependent and the independent variables. The empirical models developed (Table 3.8) were simulated using the Signal Processing toolbox of MATLAB 2008a. The graphical illustration of the simulation on each of the link was shown in Figure 3.8. The flowchart demonstrating the program input and output was shown in Figure 3.9. The simulation clearly demonstrated a linear relationship between the rainfall rate and the induced rain attenuation.

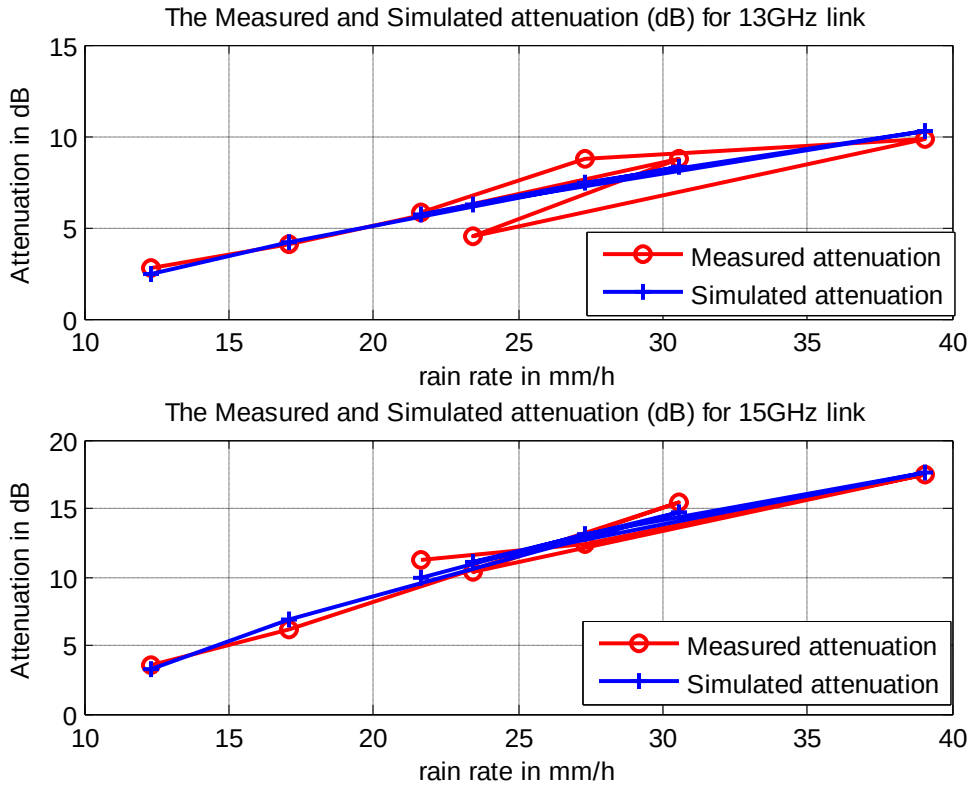

Figure 3.8:Simulations of the Developed Models

3.5.4 Flow Chart of the Program

The program initializes with clear screen followed by the input data. The data include the average monthly rain rate (R_p), the clear sky measured RSL and the RSL measured during the rain conditionfor the seven months of rainfall. The polynomial function computes the predicted rain induced attenuation or elsethe link performance analysis is documented as a measured rain induced attenuation. The program runs through the seven months of available processed input (Rain Rate) and display theoutput appropriately as the predicted rain induced attenuation, A_p. When the input data is less than seven (within rainfall period), a graph of the predicted rain induced attenuation and the rain rate is plotted; else, the system displaysthe discounted RSL value as the measured rain attenuation and plot the graph. Otherwise, the result is reprocessed for a predicted attenuation.

The graph for the plot of the rain rate and the predicted attenuation shows a deterministic linear graph whose mean error and standard deviations were known.The Root Mean Square Error and the Mean Model Error are computed with respect to the measured rain induced attenuation A_m. The coefficient of the linear graph is unity because of the system approximation. The flow chart of the program simulation is shown in figure 3.9.

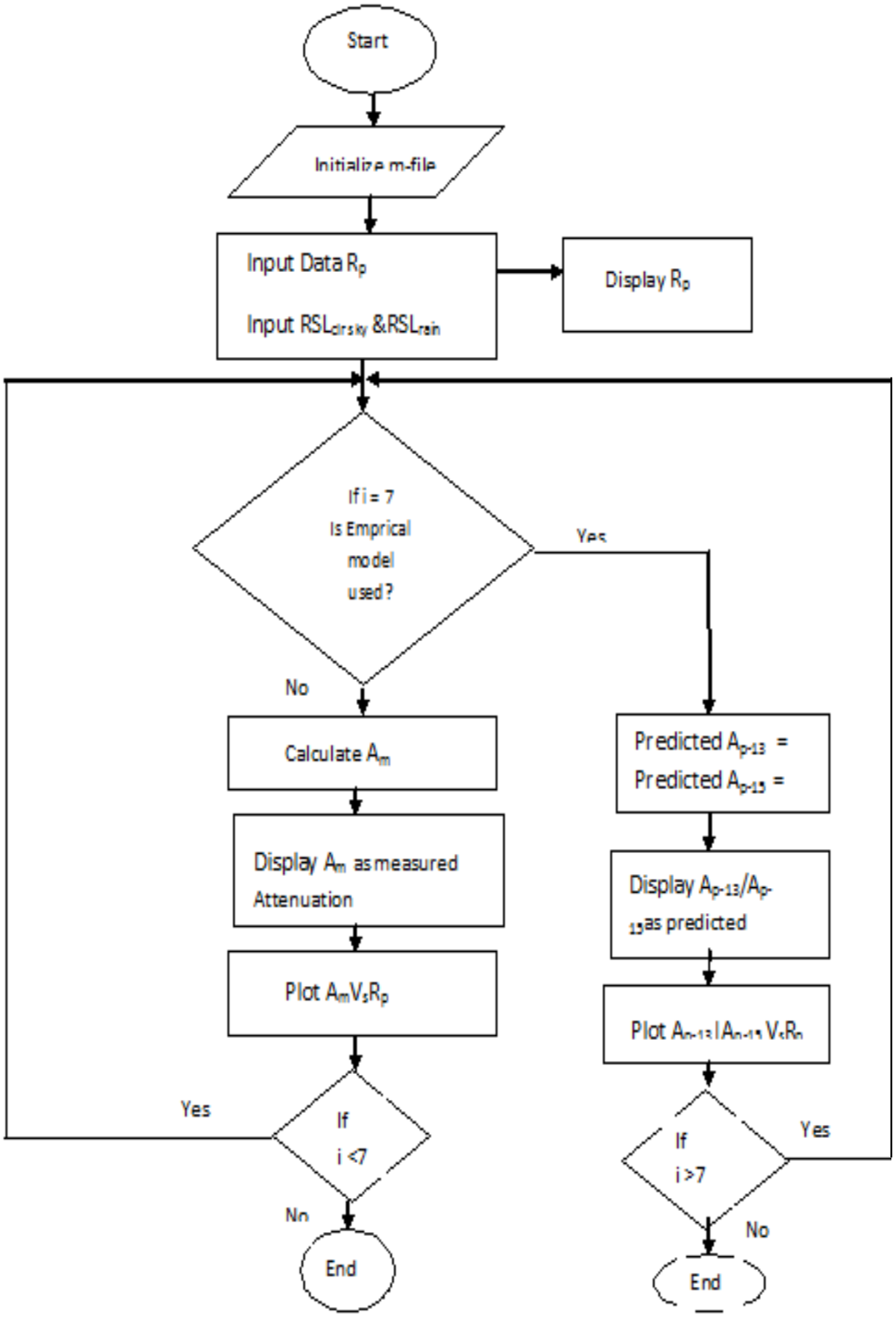

Figure 3.9: Flowchart for Rain Induced Attenuation Program

3.6 Model Validation

The empirical model developed was validated using the ITU-R terrestrial attenuation model. There were a number of acceptable existing model like the Moupfoum attenuation model for the tropical climate, Olsen and Crane rain attenuation for the tropical region of the world. The basic difference in the approaches of these models was in the determination of the link effective path loss. However, all the models are modifications to the ITU-R specific rain attenuation model. In this research, the ITU-R terrestrial rain attenuation model was adopted for the validation of the predicted empirical model.

3.6.1 Test of the Predicted Model

Further to the statistical evaluation of the developed model, the extracted rain rate (R_P)for2009 and 2010 in table 3.1was used as the varied input for the model test. The developed model prediction result is shown in Table 3.9.

Table 3.9: Rain Attenuation Prediction using the Developed Model

Months	Predicted Attenuation (dB) 2009		Predicted Attenuation (dB) 2010	
	13GHz	15GHz	13GHz	15GHz
April	0.18	2.20	4.64	7.85
May	3.42	5.38	4.90	8.36
June	6.79	11.98	9.62	16.74
July	4.16	6.88	8.13	14.37
August	11.35	18.78	8.74	15.38

September	4.98	8.53	9.43	16.46
October	5.81	10.12	5.65	9.82

The prediction result from the test models indicated a trend of proportionality with the rain rate (R_p). The model generally predicted higher attenuation for 2010-rain season than for 2009. However, August 2009 with the highest rain rate of 45.95mm/h equally had the highest predicted attenuation. The model estimated 11.35dB for the 13GHz microwave link and 18.78dB for the 15GHz link in the same month of August 2009. The developed model test result obtained was required for validation using the ITU-R terrestrial rain attenuation model.

3.6.2 The ITU-R Rain Attenuation Model

The developed polynomial functions (Table 3.8) evaluated and tested was validated using the ITU-R terrestrial Rain Attenuation model. The ITU-R model equation 2.1 expresses rain attenuation calculation to availability at (0.01%) percentage of time of the year. Consequently, the rain rate at 0.01% ($R_{0.01\%}$) was determined using equation 2.14. In accordance with the step by step procedure of the ITU-R model as reviewed in chapter two, the rain induced attenuation $A_{0.01\%}$ was calculated. Other attenuation of the links at the $A_{0.1\%}$ and $A_{0.001\%}$ of time were computed using equation 2.19 and 2.20 subject on the link installation latitude and longitude as contained in the link document Appendix 3C. The result was shown in Table 3.8 and 3.9 for 2009 and 2010 respectively.

Table 3.10:Calculated Attenuation Using ITU-R Model Link in 2009

Rain Rate	13GHz			15GHz		
$R_{0.01\%}$ mm/h	$A_{0.1\%}$	$A_{0.01\%}$	$A_{0.001\%}$	$A_{0.1\%}$	$A_{0.01\%}$	$A_{0.001\%}$
41.03	0.61	1.59	3.39	0.84	2.21	4.72
85.13	1.42	3.73	7.96	1.92	5.04	10.75
129.75	2.33	6.10	13.02	3.10	8.10	17.29
94.44	1.61	4.21	8.98	2.16	5.66	12.09
213.47	4.17	10.91	23.29	5.43	14.21	30.33
105.11	1.82	4.77	10.18	2.44	6.39	13.64
116.03	2.05	5.35	11.43	2.73	7.14	15.25

Table 3.11:Calculated Attenuation Using ITU-R Model in 2010 Link

Rain Rate	13GHz			15GHz		
$R_{0.01\%}$ mm/h	$A_{0.1\%}$	$A_{0.01\%}$	$A_{0.001\%}$	$A_{0.1\%}$	$A_{0.01\%}$	$A_{0.001\%}$
101.13	1.74	4.56	9.73	2.34	6.12	13.06
103.99	1.80	4.71	10.05	2.41	6.31	13.47
175.17	3.31	8.66	18.49	4.34	11.31	24.26
149.83	2.76	7.22	15.40	3.64	9.53	20.34
159.61	2.97	7.77	16.58	3.91	10.23	21.85
171.62	3.23	8.46	18.05	4.24	11.11	23.71
113.89	2.00	5.24	11.18	2.67	6.99	14.93

Having computed the ITU-R attenuation$A_{p\%}$ using the ITU-R terrestrial attenuation model, a comparison of the results was made with the predicted empirical model.

Establishing high degree of agreement between the two models validates the predicted model as an empirical model for the prediction of rain induced attenuation at 13GHz and 15GHz microwave frequencies.

3.7 Summary of Chapter Three

Rainfall rate was extracted from the collected NIMET data and the attenuation due to rainfall measured directly from link received signal level. Theoretical modeling was made to producedifferentempirical models or curve fitting functions using least square method implemented by Microsoft Excel Trend-line chart approach. The best curve fitting function among the set of equations developed was identified by the regression coefficient values and further evaluated for acceptance using chi-square test and root mean square error statistical techniques. Polynomial curve fitting functions had the lowest root mean square error (RMSE) of 0.86 and 0.73 for the 13 and 15GHz microwave frequencies and was presented as the developed empirical model.

CHAPTER FOUR

RESULTS AND DISCUSSION

4.1 Introduction

This research work employed both statistical and semi-empirical approach for the development of prediction model using the direct attenuation measurement obtained from the links. The rain rate used was extracted from the NIMET rain data obtained for the period of 2009 and 2010 rain season. Each year witnessed more than 90-rain events with higher rainfall and rainfall rate in 2010. However, August 2009 had the highest measured rain rate of 213.47mm/h at ITU-R 1-minute integration time. This suggests wrong categorization of Nigeria to P zone of the ITU-R rain contour map with an assumed rain rate of 145mm/h. This error is one of the fundamental reasons why the ITU-R model prediction has to be modified. The rainfall effects on the links accounted for the result obtained in the analysis of the links fade margin.

In chapter three the predicted models estimated for higher rain attenuation values than the ITU-R model. The results obtained from the two were presented in this chapter and the comparison made for the values were shown graphically in Figure 4.1 and Figure 4.2. The predicted models were simulated using MATLAB R2008a Figure 3.10. The simulation results showed the model linearity, the curve regression coefficient, mean model error and standard deviation. The flow chart for the program input and out was illustrated in Figure 3.9.

4.2 Rain Intensity Analysis

The rain statistics Figure 3.5 shows that the rainfall $R_p$rate was generally higher in 2010 except for August 2009 with 45.95mm/h rain rate. The mean rain rate estimated for the two years also shows higher rain rate for August as indicated in table 4.1. The table also showed the estimated rain rate at the ITU-R 0.01% of time using equation 2.14. The calculated rain rate $R_{0.01\%}$of 213.47mm/h in August indicated a huge under estimation for rain rate by the ITU-R when compared with the 145mm/h recommended value for Nigeria in the P categorization on the rain map Appendix 2B and Table 2.2

Table 4.1: Rain Rate at 1-Minute Integration Time

Months	2009 Rain Rate (mm/h)		2010 Rain Rate (mm/h)	
	R_p (Data)	$R_{0.01\%}$	R_p	$R_{0.01\%}$
April	6.16	41.03	18.39	101.13
May	14.99	85.13	19.13	103.99
June	25.05	129.75	36.11	175.17
July	17.01	94.44	29.85	149.83
August	45.95	213.47	32.24	159.61
September	19.38	105.11	35.22	171.62
October	21.86	116.03	21.37	113.89

4.3 Rain Induced Attenuation

The rain induced attenuation values for each of the links was measured on monthly basis within the period of the two rainy seasons. The measured data Table 3.5 indicated a direct

proportionality with the rain rate obtained Table 3.1. The 13GHz microwave link had the highest excess mean rain attenuation of 9.89dB in August when the rainfall is high. The 15GHz link had 17.52dB excess attenuation due to rainfall at the same period. The ITU-R model in Table 3.8 and 3.9 showed under estimation for excess attenuation of the two links at0.1% and 0.01% of time. The model result was used to validate the developed model (Table 3.09) on test using the varied rainfall obtained for 2009 and 2010 rain season. The developed empirical model predicted highest rain attenuation of 11.35dB for the 13GHz and 18.78dB for the 15GHz microwave link.

Figure 4.1and Figure 4.2 showed the developed model and the ITU-R model to be in close agreement even though the ITU-R model under estimated at 0.01% of time. The ITU-R model estimated 10.91dB for the August 2009 high rainfall when the developed model predicted 11.35dB for 13GHz microwave link. In the same period the ITU-R model estimated 14.21dB for the 15GHz frequency against 18.78dB predicted by the developed model at 0.01% of time.

The ITU-R model clearly over estimated for the rain attenuation of all the links at 0.001% of time with excess estimate of 23.29dB and 30.33dB for the 13GHz and 15GHz frequencies respectively.

4.4 Comparison of the Predicted Models with the ITU-R Model

Generally the ITU-R model predicted lower at both 0.1% and 0.01% time of the year. This means that the ITU-R model under estimated for the rain induced attenuation for the two microwave links in Kaduna. The model however, shows close agreement with the predicted values of both 13GHz and 15GHz frequency at 0.01% time but at variance for

over estimation at 0.001% of time. The developed empirical model predicted highest rain attenuation of 11.35dB for the 13GHz and 18.78dB for the 15GHz microwave link while the ITU-R model gave 10.91dB excess attenuation values at the 13GHz and 14.21dB at 15GHz link as shown in Figure (4.1) and Figure (4.2)

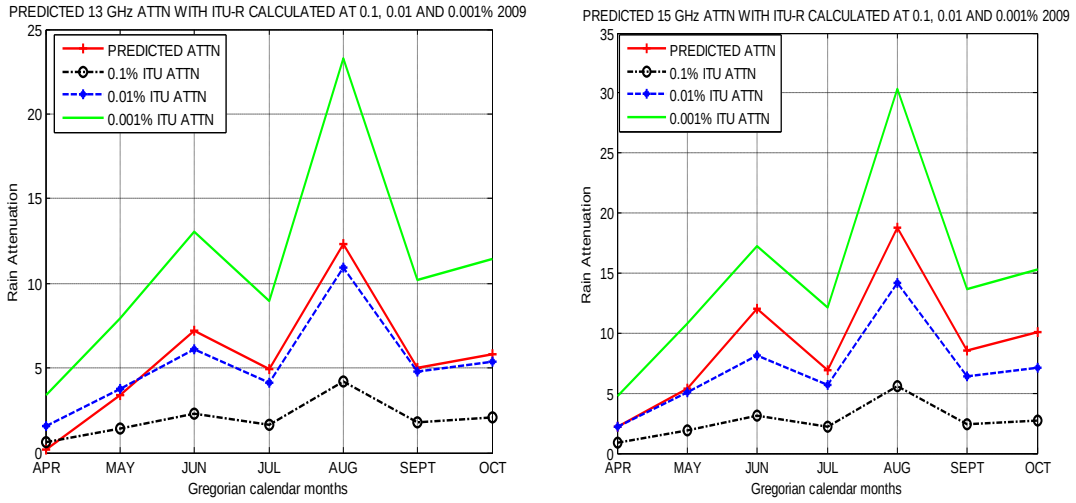

Figure 4.1: Comparism of predicted attenuation with ITU-R model in 2009

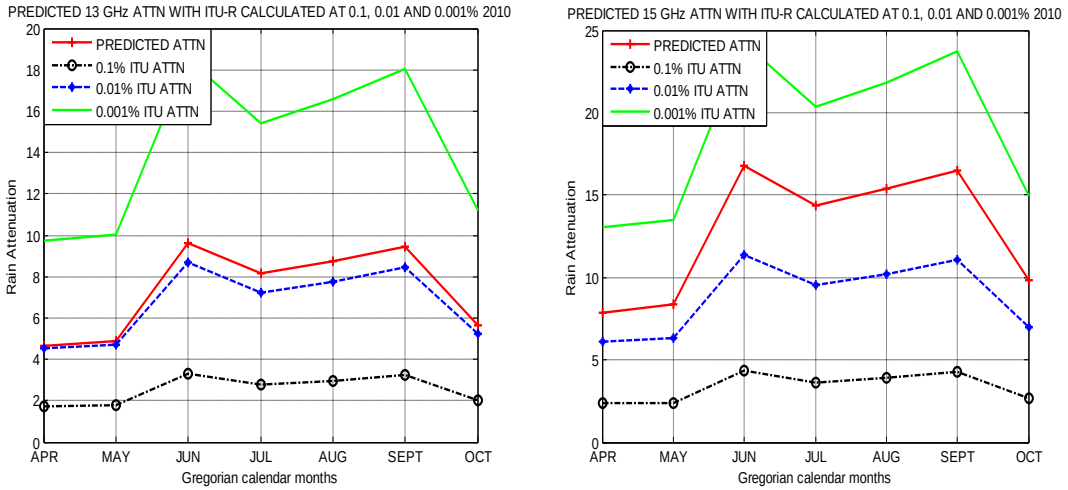

Figure 4.2: Comparism of predicted attenuation with ITU-R model in 2010

Figure 4.2 further showed that the ITU-R model under estimated for rain induced attenuation increased with the increase in rainfall in 2010. The ITU-R model under

estimation also show increase with frequency as compared with the measured values of 12.95dB and 19.95dB (Table 3.5) for the 13GHz and 15GHz link in August 2009. Appendix 4A is the MATLAB program for the comparison of the two models and the result showed that the predicted model had a mean error of 0.78dB and 3.02dB when compared with ITU-R model.

4.5 Matlab Program Simulation Result

The matlab program is attached as appendix 3E. The program results and code presents the model mean model error, regression coefficients, mean standard error and the standard deviation.The simulation results showed a mean model error (MME) of 0.00190 for the 13GHz with standard deviation (SD) of 0.0043 while the 15GHz showed a mean model error (MME) of 0.01079 with 0.0245 as its standard deviation (SD) value. The normalized functions has a gradient (m) of 0.2926 with an intercept (C) of -0.7947 for the 13GHz predicted function while the 15GHz has the slope (m) of 0.5342 and the intercept (C) of -2.1496. Figure 3.8 also confirmed the theoretical assumption of linearity and direct proportionality between the dependent and the control variables.

The predicted attenuation, Ap_13=2.39 dB

The predicted attenuation, Ap_13=4.17 dB

The predicted attenuation, Ap_13=8.32 dB

The predicted attenuation, Ap_13=6.30 dB

The predicted attenuation, Ap_13=10.22 dB

The predicted attenuation, Ap_13=7.44 dB

The predicted attenuation, Ap_13=5.73 dB

The predicted attenuation, Ap_15=3.26 dB

The predicted attenuation, Ap_15=6.90 dB

The predicted attenuation, Ap_15=14.67 dB

The predicted attenuation, Ap_15=11.05 dB

The predicted attenuation, Ap_15=17.55 dB

The predicted attenuation, Ap_15=13.14 dB

The predicted attenuation, Ap_15=9.96 dB

The rain rate, Rp=12.325 mm/h

The rain rate, Rp=17.060 mm/h

The rain rate, Rp=30.580 mm/h

The rain rate, Rp=23.430 mm/h

The rain rate, Rp=39.095 mm/h

The rain rate, Rp=27.300 mm/h

The rain rate, Rp=21.615 mm/h

The Measured attenuation, Am_13=2.72 dB

The Measured attenuation, Am_13=4.09 dB

The Measured attenuation, Am_13=8.78 dB

The Measured attenuation, Am_13=4.52 dB

The Measured attenuation, Am_13=9.89 dB

The Measured attenuation, Am_13=8.75 dB

The Measured attenuation, Am_13=5.82 dB

The Measured attenuation, Am_15=3.52 dB

The Measured attenuation, Am_15=6.15 dB

The Measured attenuation, Am_15=15.42 dB

The Measured attenuation, Am_15=10.42 dB

The Measured attenuation, Am_15=17.52 dB

The Measured attenuation, Am_15=12.32 dB

The Measured attenuation, Am_15=11.25 dB

The model error, err_13=0.33 dB

The model error, err_13=-0.08 dB

The model error, err_13=0.46 dB

The model error, err_13=-1.78 dB

The model error, err_13=-0.33 dB

The model error, err_13=1.31 dB

The model error, err_13=0.09 dB

The model error, err_15=0.26 dB

The model error, err_15=-0.75 dB

The model error, err_15=0.75 dB

The model error, err_15=-0.63 dB

The model error, err_15=-0.03 dB

The model error, err_15=-0.82 dB

The model error, err_15=1.29 dB

MSE_13 is 0.0016

MSE_15 is 0.0092

RMSE_13 is 0.0403

RMSE_15 is 0.0962

Mean model error_13 =-0.00190

Mean model error_15 =0.01079

R is 171.4050

SD_13 is 0.0043

SD_15 is 0.0245

coefficient of correlation_13 is 1.0000

coefficient of correlation_15 is 1.0000

Gradient of Predicted Model at 13GHz is 0.2926

Y intercept of Predicted Model at 13GHz is -0.7947

Gradient of Predicted Model at 15GHz is 0.5342

Y intercept of Predicted Model at 15GHz is -2.1496

4.6 Summary of Chapter Four

The attenuation measurement due to rainfall was obtained directly and it was also predicted using theoretical modeling approach. Firstly, the links recorded unavailability of service at some instant of rainfall when the signal fade margin of -80dBm and -77dBm were recorded by the 15GHz and 13GHz link respectively. The theoretical developed models were the polynomial curve fitting functions becausethe two had the lowest root mean square error (RMSE) of 0.86 and 0.73 for the 13 and 15GHz microwave frequencies. The developed empirical model predicted 11.35dB as the highest attenuation induced by rain for the 13GHz link and 18.78dB for the 15GHz in the same period. These high values of attenuation due to rain had to be compensated for in the link budget to make the links available throughout the year.

CHAPTER FIVE

CONCLUSION AND RECOMMENDATIONS

5.1 Conclusions

The objectives of this research work are all achieved. Theoretical empirical models for both 13GHz and 15GHz microwave frequencies were developed. The model development was based on direct measurement of received signal levels of the links.It can be observed from the research work Figure 3.8 that the developed empirical models showed direct linear proportionality between the rain rate and the rain induced attenuation. The model also showed that attenuation due to rainfall increased with frequency.Themodel predicted high attenuation level for each of the links and concluded that the attenuation value could cause service unavailability at 0.01% of time.TheMatlab simulation puts the coefficient of correlation at unity due to approximation. The mean model error is 0.0019dB and 0.0108dB for 13GHz and 15GHz link respectively. The graphs however, showed that the ITU-R model under estimatedfor the rain induced attenuation of the links even at 0.01% of time. When the rainfall was heavy between Junes to September the 15GHz link showed more variation with ITU-R model even at 0.01% of time. The developed empiricalmodel was clearly at variance with the ITU-R prediction at 0.1%, and 0.001% of time, but showed relatively closeagreement at light rainfall at 0.01% of time. These developed models proposed in this work can be used directly to determine attenuation caused by rain at 13GHz and 15GHz microwave frequencies.

5.2 Limitations

The predicted empirical models proved to give more precise rain induced attenuation results when compared with the ITU-R model for the 13GHz and 15GHz microwave frequencies. The model dependent variable is limited to the rainfall rate only. This limitation may subject the model to criticism for not accounting for certain climatic considerations defined by the ITU-R parameter a and b in the model equation ($A_p = aR_p^b(d_{eff})$) until the constants of the polynomial functions are investigated.

5.3 Recommendations

The high rain rate predictedan impairment of 11.35dB on the 13GHz and 18.78dB on the 15GHz link. It is therefore recommended that fade mitigation techniques (FMT), either adaptive or control type be implemented on the links to limit the rain attenuationeffect, and maintain service availability for the microwave link even during anyrain events.

REFERENCES

Abdullah H; Abdullah M. and Y.Y, Ng; (2010), The study of rain specific attenuation for the prediction of satellite propagation in Malaysia, *Journal of infrared, Millimeter, and Terahertz waves31(6)/681- 689.*

Agilent Technologies, GSM Fundamentals(copyright2000),*10001633-GSM Fund.ppt Rev5/16/00*,http://mars.tekkom.dk/mediawiki/images/8/88/GSM_praesentation_noter.pdf.

Agunlejika O; Raji T.I and Adeleke A.O (2009) Tropospheric Scintillation Prediction for Some Selected Cities in Nigeria's Tropical Climate,*International Journals of basic and applied Sciences 09(10)*

Ajayi G.O, Ajewole M.O and Kolawole L.B (1999) Theoretical study of the effect of different types of tropical rainfall on microwave and millimeter wave propagation,*Radio Science Journal, 34(5)/1103-1124.*

Alonge A. and Afullo T.J.O (2012) Seasonal analysis and prediction of rainfall effects in Eastern South Africa At microwave frequencies,*progress in Electromagnetics Research B, 40/279-303*

Ashish, S. and Prashant, J. (2010),Effect of Rain on Radio Propagation in GSM,*International Journal of Advanced Engineering and Application, /2-4*

Crane, R.K. (2003)Propagation Hand Book for Wireless Communication System Design, *The Electrical Engineering and Applied Signals Processing Series, CRC press, New York,*

Das S. Maitra A., and ShuklaA.k (2010), Rain-induced attenuation modeling in the 10-100Ghz frequency using drop size distribution for different climatic zones in tropical india, *progress in Electromagnetic Research B, 25/211-224.*

Flavin R.K (1981), Rain attenuation considerations for satellite paths, *Telecommunication Australia Research laboratories, Report(7505).*

Folaponmile A and Sani M.S; (2011), Empirical Model for the Prediction of Mobile Radio Cellular Signal Attenuation in Harmattan Weather,*Information Technology Research Journals, 1 (1)/13-20*

Forknall, N; Cole, R and Webb, D; (2008),Cumulative fading and rainfall distribution for a 2.1km, 38GHz, vertically polarized, Line of Sight (LOS) link,*IEEE Transport andAntenna propagation 56(4)/1085-1093.*

Freeman R. (1997), Radio System Design for Telecommunications, *John Wiley and Sons, 2nd Edition, /468-471.*

GSM Architecture and Interfaces (1998), GSM 05/71-90www.pearsonhighered.com/samplechapter/0139491244.pdf.

Hall M (1981), Dual Polarization radar helps gauge rainfall rate, *Microwaves 20(9)/93-101*

Isikwue B.C, Ikayo A.H and Utah E.U; (2013), Analysis of Rainfall Rate and Attenuation for LOS EHF/SHF Radio Communication Links over Markurdi, Nigeria, *Research Journal of Earth and planetary Science, 3(2)/60-74*

Islam M.R, and Rahman T.A. (2009), Fade margins prediction for Broadband fixed wireless access (BFWA) from measurements in tropics, *Progress in electromagnetic Research C, 11/199-212.*

Intelsat, (2006), Antenna and wideband RF performance characteristics of ku-band earth stations accessing the Intelsat space segment for standard services, *Intelsat earth station standards, IESS-208 (Rev.6)*

ITU-R, 838-3 (2005), Specific attenuation model for rain for use in prediction methods, *Recommendation, ITU-R P, Question ITU-R 201/3*

ITU-R, 530-12 (2007), Propagation data and prediction methods required for the design of terrestrial line of sight systems, *Recommendation, ITU-R P, Question 204/3*

ITU-R, 837-4 (2007), Characteristics of precipitation for propagation modeling, *Revision of recommendation, Document 3/111 (Revision 1)*

Khairayu B; Ahmad F.I; Jafri D. and Abdul-Rahman T; (2011), Rain induced attenuation studies for V-band satellite communication in tropical region, *Journal of atmospheric and solar-terrestrial physics, 73/601-610*

Lam, H.Y; (2010),Application of the SC EXCELL model for rain induced attenuation prediction in tropical and equatorial regions,*IEEE Asia Pacific Conference on Applied Electromagnetic, APACE 2010, proceedings, art no- (5720079)/1-6*

Matricciani E, and Pawlina-Bonati (2000), Statistical characterization of rainfall structures and occurrence for convective and stratiform rain inferred from long-term point rain rate data. *AP-2000 millennium conference on antenna propagation, Davos, /9-14*

Matzler C, (2002b), Drop size distributions and mie computations for rain, *IAP research report, 2002(16)*

Moupfouma F.(2009), Electromagnetic wave attenuation due to rain, A precipitation model for terrestrial or line of sight SHF and EHF radio communication links, *Journal of Infrared, millennium Tetrahertz waves, 30(2)/622-632*

Odedina, M.O., and Afullo,T.J, (2007). Modeling of Rain attenuation for terrestrial LOS radio system in South Africa, *Proceeding of southern Africa telecommunications Network Applications conference (SATNAC), satnac.org.za*

Ofoche E.B.C and Ajayi G.O (1983), Some tropical rainfall rate characteristics at Ile-Ife for microwave and millimeter wave applications, *Journal of Climate and Applied Meteorology, 23/562-567*

Oguchi T. (1973), Attenuation and Phase rotation of radio waves due to rain: Calculation at 19.3 and 34.8GHz, *Radio Science Journal, 8(1)/31-38*

Ojo J.S and Ajewole M.O (2008), Rain rate and rain attenuation prediction for satellite communication in KU and KA bands over Nigeria, *Progress in electromagnetic research, 5/207-223.*

Olsen R.L and Ajayi G.O. (1999), Modeling of a tropical rain drop size distribution for microwave applications, *Radio Science. 20/193-202.*

Olsen R.L, Regers D.V and Hodge D.B (1978), The aR^b relation in the calculation of rain attenuation, *IEEE Transaction and Antenna Propagation 26(2)/547-556*

Oluwafemi C.O and Omotosho T.V; (2009), Impairment of radio wave signal by rainfall on fixed satellite service on earth space path at 37 stations in Nigeria,*Journal of Atmospheric and Solar Terrestrial physic 71issue (8-9)/830-840.*

Omotosho T.V and Oluwafemi C.O; (2009), One minute rain rate distribution in Nigeria from Tropical Rainfall Measuring Mission (TRMM) satellite data, *Journal of Atmospheric and Solar Terrestrial physics,71 Issue (5)/625-633.*

Owolawi, P.A., and Afullo, T.J, (2007), Rainfall rate modeling and worst month statistics for millimetric Line of sight radio links in South Africa,*Radio Science Journal, 42, Issue (6),doi(10), RS6004.*

Parshotam S; Interjit S.H, and Maninder L.S, (2011),Estimation of path length reduction factor by using one year rain attenuation statistics over a line of sight (LOS) link operating at 28.75GHz in Armristar (INDIA),*Journal for infrared, millimeter, and Tetraherz waves, (32) issue (2)/137-142.*

Radio-Electronics. Resources and analysis for electronics engineers.http://www.radio-electronics.com/info/cellulartelecomms/gsm_technical/gsm_interfaces.php

Ray H; (2007), Telecommunications and data communications handbook, *Wiley Interscience,ISBN 978-0-47—04141-3, /476.*

Rec. ITU-R PN.676-1, (1992), Attenuation by atmospheric gases

Segal B. (1986), The Influence of Raingauge integration time on measured rainfall intensity distribution functions, *Journal of Atmospheric and oceanic Technology, 32/662-671.*

Seker S.S and Kunter F; (2013), Simulation of discrete electromagnetic propagation model for atmospheric effects on mobile communication, *Turkish Journal of Electrical Engineering and Computer Science, elk-1204-12.*

Watson P.A, Sathiaseelan and Potter B (1981), Development of Climate map of rainfall Attenuation for Europe, *UK, Report,(300)/134-141*

Zhang W. and Moanyeri N. (1999), Power-Law parameters of rain specific attenuation, *Broadband Wireless Access Working Group, IEEE 802.16 99/41*

APPENDIX 2A

ITU-R Specific Rain Attenuation Parameters

Frequency (GHz)	k_H	α_H	k_V	α_V
1	0.0000259	0.9691	0.0000308	0.8592
1.5	0.0000443	1.0185	0.0000574	0.8957
2	0.0000847	1.0664	0.0000998	0.9490
2.5	0.0001321	1.1209	0.0001464	1.0085
3	0.0001390	1.2322	0.0001942	1.0688
3.5	0.0001155	1.4189	0.0002346	1.1387
4	0.0001071	1.6009	0.0002461	1.2476
4.5	0.0001340	1.6948	0.0002347	1.3987
5	0.0002162	1.6969	0.0002428	1.5317
5.5	0.0003909	1.6499	0.0003115	1.5882
6	0.0007056	1.5900	0.0004878	1.5728
7	0.001915	1.4810	0.001425	1.4745
8	0.004115	1.3905	0.003450	1.3797
9	0.007535	1.3155	0.006691	1.2895
10	0.01217	1.2571	0.01129	1.2156
11	0.01772	1.2140	0.01731	1.1617
12	0.02386	1.1825	0.02455	1.1216
13	0.03041	1.1586	0.03266	1.0901
14	0.03738	1.1396	0.04126	1.0646
15	0.04481	1.1233	0.05008	1.0440
16	0.05282	1.1086	0.05899	1.0273
17	0.06146	1.0949	0.06797	1.0137
18	0.07078	1.0818	0.07708	1.0025
19	0.08084	1.0691	0.08642	0.9930
20	0.09164	1.0568	0.09611	0.9847
21	0.1032	1.0447	0.1063	0.9771
22	0.1155	1.0329	0.1170	0.9700
23	0.1286	1.0214	0.1284	0.9630
24	0.1425	1.0101	0.1404	0.9561
25	0.1571	0.9991	0.1533	0.9491
26	0.1724	0.9884	0.1669	0.9421
27	0.1884	0.9780	0.1813	0.9349

Appendix 2B

ITU-R Rain Climatic Region: Map for Africa & Europe

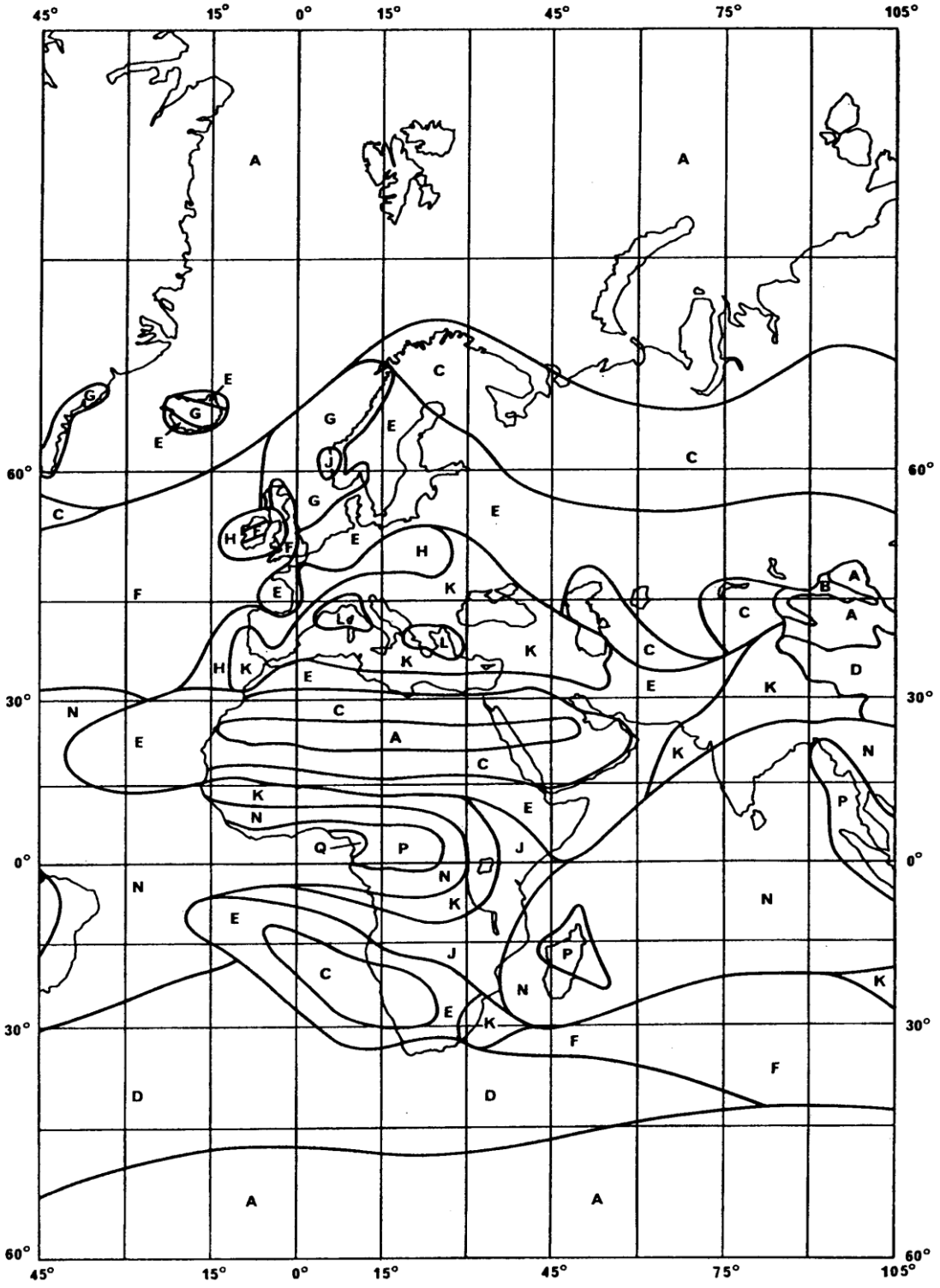

APPENDIX 3A

NIMET RAINFALL DATA FOR KADUNA-NIGERIA

CALCULATED RAIN RATE FROM NIMET DATA FOR 2010 RAIN SEASON

APRIL 2010

DATE	RAINFALL (mm)	DURATION (min)	Rain Rate (mm/h)
16	0.2	23	0.52
24	13.5	22	36.81
26	5.6	18	18.66
29	10.5	26	24.23
30	4.1	21	11.71
		Mean Rain Rate (mm/h)	**18.39**

MAY 2010

DATE	RAINFALL (mm)	DURATION (min)	Rain Rate (mm/h)
5	1.4	21	4
6	25.6	19	80.84
11	11.1	15	44
17	0.2	32	4
19	6.6	19	0.37
20	0.3	10	20.84
21	1	14	1.8
23	0.9	10	4.28
28	13.3	23	5.4
29	0.6	13	34.69
31	1.5	20	2.76
			4.5
		Mean Rain Rate (mm/h)	**19.13**

JUNE 2010

DATE	RAINFALL (mm)	DURATION (min)	Rate Rate (mm/h)
4	21.9	42	31.28
5	28.7	18	95.66
8	0.2	13	0.92
9	1	17	3.52
10	35	16	131.25
13	12.3	21	35.14
14	1.5	26	3.46

16	4.8	31	9.29
17	0.1	19	0.31
20	13.2	32	2475
21	28.7	23	74.82
25	36.5	24	91.25
26	12.4	32	23.25
27	6.5	23	16.95
		Mean Rain Rate (mm/h)	**36.11**

APPENDIX 3A (CONTINUE)

JULY 2010

DATE	RAINFALL (mm)	DURATION (min)	Rain Rate (mm/h)
1	23.5	35	40.28
6	22.6	46	29.47
7	12.3	26	28.38
8	15	19	47.36
9	19.2	22	52.36
14	1.5	15	6
15	4.4	19	13.89
16	5.5	16	20.62
17	0.2	33	0.36
20	31.1	22	84.81
21	4.8	18	16
22	2.5	15	10
23	26.7	21	76.28
24	3	16	11.25
27	5.5	16	20.62.
30	1.8	14	7.71
31	5.5	19	17.36
Mean Rain Rate (mm/h)			**29.85**

AUGUST 2010

DATE	RAINFALL (mm)	DURATION (min)	Rain Rate (mm/h)

1	1.6	14	6.85
2	1.6	21	4.57
3	4.3	24	10.75
5	27	31	52.25
5	0.4	58	0.44
7	0.2	12	
8	4.8	33	
9	37.2	19	
11	5.1	11	
12	69.9	103	
13	3.4	10	
14	23.8	14	
19	5.2	13	
20	22.5	16	
21	17.5	63	
23	19.8	43	
24	3.3	36	
25	34.3	15	
26	18.3	30	

Mean Rain Rate (mm/h) **32.24**

APPENDIX 3A (CONTINUE)
SEPTEMBER 2010

DATE	RAINFALL (mm)	DURATION (min)	Rain Rate (mm/h)
1	1.2	11	6.54
2	27.6	34	48.70
4	18	15	75.2
6	37.3	15	149.2
8	16	12	80
9	4.8	41	7.02
13	10.6	28	22.71
14	23.1	16	86.62
16	7.3	17	25.76
17	2.1	9	14

19	27.8	19	87.78
24	40.1	129	18.65
28	32.3	78	24.76
Mean Rain Rate (mm/h)			**35.22**

OCTOBER 2010

DATE	RAINFALL (mm)	DURATION (min)	Rain Rate (mm/h)
2	1.9	7	16.28
4	12.3	32	22.87
5	4.3	49	5.26
6	38.8	109	21.35
7	3	10	18
10	5.8	19	18.31
11	13.8	33	25.09
15	3.8	13	17.55
18	5.3	21	15.14
19	15.5	12	77.5
21	21.5	38	33.94
23	11.6	43	16.18
24	10.2	21	29.14
25	1.5	12	7.5
Mean Rain Rate (mm/h)			**21.37**

CALCULATED RAIN RATE FROM NIMET DATA FOR 2010 RAIN SEASON

APRIL 2009

DATE	RAINFALL (mm)	DURATION (min)	Rain Rate (mm/h)
4	4.7	44	6.40
19	1.8	38	2.84
20	3.9	54	4.33
21	0.2	29	0.41
25	15.8	92	10.30
Mean Rain Rate (mm/h)			**6.16**

APPENDIX 3A (CONTINUE)

MAY 2009

DATE	RAINFALL (mm)	DURATION (min)	Rain Rate (mm/h)
2	4.9	31	9.48
4	2.2	17	7.76
8	3.5	51	4.11
14	13.8	44	18.81
16	12.3	30	24.6
24	12.5	19	39.47
25	3.5	22	9.54
29	10.5	39	16.15
Mean Rain Rate (mm/h)			**14.99**

JUNE 2009

DATE	RAINFALL (mm)	DURATION (min)	Rain Rate (mm/h)
3	13.2	18	44
4	8.5	38	13.42
5	8.2	51	9.64
7	14.8	33	26.90
9	43.2	31	83.61
15	6.5	29	13.44
18	4.5	37	7.29
20	14.6	69	12.69
25	18	22	49.09
28	13.7	24	34.25
30	12.2	25	29.28
Mean Rain Rate (mm/h)			**25.05**

JULY 2009

DATE	RAINFALL (mm)	DURATION (min)	Rain Rate (mm/h)
3	16.8	39	25.84
5	0.7	139	0.30
8	12.5	73	10.27
11	3.3	21	9.42
12	30.4	42	43.42
13	1.6	31	3.09

16	34.5	82	25.24
20	5	24	12.3
22	0.3	12	1.5
23	1.5	23	3.91
25	2.7	18	9
26	0.5	12	2.5
27	8.7	25	20.88
29	28.8	35	49.37
30	34.7	66	31.54
Mean Rain Rate (mm/h)			**17.01**

APPENDIX 3A (CONTINUE)

AUGUST 2009

DATE	RAINFALL (mm)	DURATION (min)	Rain Rate (mm/h)
2	59	48	73.75
5	27.6	44	37.90
7	14.4	39	22.15
8	2.2	22	6
9	7.9	28	16.92
11	12.2	40	18.3
12	47.1	69	40.95
13	0.8	23	2.08
14	23.4	19	73.89
15	12.8	36	21.33
16	15.7	47	20.04
17	5.5	30	11
18	23.6	40	35.4
19	2.6	31	5.03
20	17.3	19	54.63
22	3.6	18	12
24	18.9	32	35.43
25	51.3	57	54
27	35.1	77	27.35
28	40	119	20.16
30	38.5	89	25.95

Mean Rain Rate (mm/h)			**45.95**

SEPTEMBER 2009

DATE	RAINFALL (mm)	DURATION (min)	Rain Rate (mm/h)
2	4.1	32	7.68
4	22.5	22	61.36
5	0.1	11	0.54
6	16.6	43	23.16
8	0.3	18	1
11	0.2	18	0.67
12	14.8	63	14.09
14	5	39	7.69
15	5.3	27	11.78
16	0.1	11	0.55
17	19.9	15	79.6
19	12.2	23	39.83
20	14	20	42
21	0.9	21	2.57
24	0.3	11	1.63
27	13	22	35.45
28	4.1	17	14.47
Mean Rain Rate (mm/h)			**19.38**

APPENDIX 3A (CONTINUE)

OCTOBER 2009

DATE	RAINFALL (mm)	DURATION (min)	Rain Rate (mm/h)
2	16	23	41.73
3	2.2	33	4
4	28	28	60
7	2	15	8
10	68.4	157	26.14
20	2.2	14	9.42
22	4.4	33	8
23	4.2	24	10.5
24	18	17	6.35

28	20.9	81	15.48
30	27.7	63	26.38
Mean Rain Rate (mm/h)			**21.37**

Appendix 3B

RSL CAPTURED DATA

13GHz LINK IDENTITY
Terminal ID A030, Access ID MMU 2D, Monitor RAU 2x 13/16, Reception from TX21

MEASUREMENT USING WINDOW BASED SOFTWARE: MINI-CRAFT 2.13V

S/N	April 30th 2009 RSL (dBm)	April 24th and 26th 2010 RSL (dBm)	May 8,14 and 24th 2009 RSL (dBm)	May 6,11,19 and 31st 2010 RSL (dBm)
1	-53	-55	-56	-66
2	-53	-57	-56	-63
3	-53	-57	-56	-58
4	-53	-57	-58	-58
5	-55	-52	-58	-58
6	-55	-52	-56	-59
7	-55	-55	-56	-62
8	-55	-55	-56	-62
9	-55	-55	-53	-64
10	-56	-55	-53	-61
11	-56	-55	-55	-55
12	-56	-58	-55	-55
13	-56	-58	-55	-55
14	-55	-58	-54	-56
16	-55	-57	-54	-56
17	-55	-56	-54	-57
18	-54	-56	-55	-57
19	-54	-56	-55	-57
20	-54	-58	-55	-58
21	-54	-58	-57	-56
22	-54	-58	-57	-56
23	-56	-57	-60	-56
24	-57	-55	-57	-56
25	-57	-55	-54	-59
26	-57	-55	-54	-59

27	-54	-55	-53	-59
28	-53	-56	-54	-56
29	-53	-57	-53	-56
30	-53	-62	-53	-56
31	-53	-55	-53	-58
Mean	**-54.53**	**-55.80**	**-55.06**	**-58.00**
Median	**-54**	**-56**	**-55**	**-57**

Appendix 3B Continue

Terminal ID A030, Access ID MMU 2D, Monitor RAU 2x 13/16, Reception from TX21

S/N	**June 7,9.20 and 25th 2009 RSL (dBm)**	**June 10, 14, 20 and 25th2010 RSL (dBm)**	**July 12, 16 and 27th 2009 RSL (dBm)**	**July 1,8,9,15,20 and 23rd 2010 RSL (dBm)**
1	-55	-59	-54	-55
2	-55	-57	-56	-55
3	-55	-57	-56	-55
4	-55	-56	-56	-55
5	-54	-59	-62	-54
6	-55	-59	-58	-55
7	-55	-59	-55	-55
8	-58	-66	-55	-58
9	-58	-62	-55	-58
10	-59	-62	-55	-59
11	-66	-62	-55	-61
12	-66	-59	-54	-63
13	-77	-58	-54	-66
14	-77	-55	-54	-66
15	-61	-57	-54	-61
16	-59	-59	-54	-59
17	-59	-59	-52	-59
18	-56	-63	-52	-56
19	-56	-59	-55	-56

20	-56	-65	-55	-56
21	-58	-65	-55	-54
22	-63	-65	-55	-54
23	-59	-65	-54	-57
24	-59	-69	-53	-55
25	-56	-68	-53	-56
26	-56	-71	-53	-56
27	-54	-71	-55	-55
28	-56	-79	-55	-56
29	-56	-76	-55	-67
30	-56	-71	-56	-67
31	-57	-69	-56	-67
32	-58	-69	-60	-67
33	-58	-63	-59	-67
Mean	**-58.73**	**-63.73**	**-55.15**	**-58.80**
Median	**-58**	**-66**	**-55**	**-58**

Appendix 3B Continue

Terminal ID A030, Access ID MMU 2D, Monitor RAU 2x 13/16, Reception from TX21

S/N	August 2,5,7, 11, 14 and 30th 2009 RSL (dBm)	August 3,5, 8, 9,14, 20, 23 and 26th 2010 RSL (dBm)	September 4,6,12 and 19th 2009 RSL (dBm)	September 2,4,6 and 24th 2010 RSL (dBm)
1	-55	-56	-64	-56
2	-62	-56	-63	-59
3	-62	-55	-65	-59
4	-62	-59	-63	-60
5	-67	-61	-63	-63
6	-67	-62	-63	-66
7	-67	-66	-59	-73
8	-63	-63	-58	-74
9	-56	-60	-60	-58
10	-56	-59	-59	-59
11	-59	-63	-59	-59
12	-59	-62	-59	-66
13	-64	-63	-61	-69
14	-69	-63	-63	-66
15	-73	-63	-66	-61
16	-76	-59	-66	-56
17	-74	-55	-66	-54
18	-77	-62	-62	-54
19	-69	-56	-56	-54
20	-63	-56	-56	-56
21	-63	-61	-65	-58
22	-63	-65	-65	-63
23	-65	-56	-56	-59
24	-59	-55	-55	-59
25	-59	-56	-56	-63
26	-58	-55	-58	-63

27	-63	-55	-58	-63
28	-66	-57	-59	-65
29	-72	-59	-63	-59
30	-76	-63	-63	-59
31	-76	-59	-64	-58
32	-72	-63	-64	-63
33	-67	-59	-63	-66
Mean	**-65.42**	**-59.27**	**-61.21**	**-61.21**
Median	**-64**	**-59**	**-59**	**-59**

Appendix 3B Continue

Terminal ID A030, Access ID MMU 2D, Monitor RAU 2x 13/16, Reception from TX21

S/N	October 2,10,22 and 28th 2009 RSL (dBm)	October 5,6,7,10,15,18,19,21 and 24th 2010 RSL (dBm)
1	-58	-62
2	-62	-61
3	-65	-56
4	-65	-54
5	-65	-54
6	-65	-54
7	-65	-62
8	-59	-62
9	-56	-58
10	-63	-61
11	-63	-55
12	-63	-54
13	-68	-54
14	-66	-56
15	-73	-56
16	-67	-61
17	-67	-56
18	-67	-56
19	-67	-59
20	-58	-59
21	-53	-64
22	-56	-63
23	-54	-59
24	-58	-55
25	-63	-59
26	-65	-56

27	-64	-56
28	-57	-62
29	-61	-64
30	-61	-61
31	-58	-55
32	-56	-55
33	-56	-55
Mean	**-58.48**	**-58.09**
Median	**-58**	**-57**

Appendix 3B Continue

RSL CAPTURED DATA

15GHz LINK IDENTITY
Terminal ID AB30, Access ID MMU 2D, Monitor RAU 2N 15/85, Reception from TX19

MEASUREMENT USING WINDOW BASED SOFTWARE: MINI-CRAFT 2.13V

S/N	April 30th 2009 RSL (dBm)	April 24th 26th 2010 RSL (dBm)	May 8, 14, 24 2009 RSL (dBm)	May 6. 11, 19 and 31st 2010 RSL (dBm)
1	-38	-43	-39	-44
2	-38	-40	-39	-44
3	-38	-41	-41	-48
4	-42	-41	-41	-48
5	-40	-39	-41	-52
6	-45	-39	-41	-49
7	-42	-40	-39	-49
8	-42	-40	-42	-49
9	-42	-40	-41	-47
10	-44	-42	-39	-46
11	-43	-43	-40	-44
12	-40	-41	-40	-41
13	-41	-41	-42	-42
14	-41	-41	-43	-39
15	-39	-41	-41	-42
16	-39	-41	-41	-44
17	-39	-41	-41	-46
18	-42	-42	-42	-46
19	-42	-38	-47	-46
20	-39	-38	-46	-45
21	-38	-41	-44	-45
22	-38	-41	-43	-41

23	-39	-40	-44	-40
24	-39	-40	-44	-44
25	-39	-40	-41	-44
26	-37	-39	-42	-43
27	-39	-37	-42	-41
28	-43	-39	-39	-41
29	-41	-42	-42	-44
30	-41	-41	-44	-44
31	-41	-39	-41	-41
32	-42	-40	-41	-41
33	-41	-40	-41	-39
Mean	**-40.26**	**-40.38**	**-41.67**	**-44.21**
Median	**-40**	**-41**	**-42**	**-43**

Appendix 3B Continue

Terminal ID AB30, Access ID MMU 2D, Monitor RAU 2N 15/85, Reception from TX19

S/N	June 7,9,20 and 25th 2009 RSL (dBm)	June 10,14,20, and 25th 2010 RSL (dBm)	July 12,16 and 27th 2009 RSL (dBm)	July 1,8,9,15,20 and 23rd 2010 RSL (dBm)
1	-50	-56	-42	-56
2	-52	-55	-43	-56
3	-49	-55	-44	-56
4	-49	-42	-42	-49
5	-49	-43	-41	-44
6	-47	-52	-42	-47
7	-46	-48	-42	-46
8	-44	-49	-40	-44
9	-51	-47	-40	-51
10	-51	-42	-42	-51
11	-51	-39	-43	-51
12	-53	-48	-41	-53
13	-56	-66	-41	-55
14	-56	-73	-39	-51
15	-56	-72	-43	-52
16	-49	-75	-42	-49
17	-44	-79	-44	-50
18	-44	-69	-41	-49
19	-43	-63	-41	-52
20	-41	-53	-42	-56
21	-41	-53-	-41	-56
22	-44	-55	-41	-49
23	-46	-53	-40	-44
24	-53	-51	-40	-53

25	-53	-49	-40	-53
26	-58	-51	-39	-58
27	-66	-53	-37	-53
28	-69	-49	-41	-56
29	-61	-47	-38	-56
30	-55	-46	-38	-56
31	-48	-44	-41	-49
32	-48	-57	-41	-44
33	-47	-59		
Mean	**-50.61**	**-54.33**	**-41.00**	**-51.41**
Median	**-50**	**-51**	**-40**	**-49**

Appendix 3B Continue

Terminal ID AB30, Access ID MMU 2D, Monitor RAU 2N 15/85, Reception from TX19

S/N	August 2,5,7,11,14 and 30th 2009 RSL (dBm)	August3,5,8,9,14, 20,23 and 26th 2010 RSL (dBm)	September 4,6,12 and 19th 2009 RSL (dBm)	September 2,4,6 and 28th 2010 RSL (dBm)
1	-66	-51	-39	-65
2	-61	-49	-42	-56
3	-56	-51	-43	-55
4	-54	-53	-43	-56
5	-54	-49	-44	-58
6	-54	-47	-43	-52
7	-56	-46	-41	-48
8	-58	-55	-41	-49
9	-63	-56	-44	-47
10	-59	-58	-46	-42
11	-59	-58	-44	-39
12	-63	-59	-43	-48
13	-61	-51	-50	-66
14	-63	-51	-42	-56
15	-66	-53	-42	-55
16	-65	-49	-41	-55
17	-76	-50	-40	-42
18	-80	-49	-40	-43
19	-76	-52	-41	-52
20	-71	-51	-43	-48
21	-65	-49	-45	-49
22	-56	-51	-41	-49
23	-55	-53	-40	-44

24	-56	-49	-39	-47
25	-58	-47	-39	-46
26	-58	-58	-39	-51
27	59	-53	-41	-57
28	-51	-56	-51	-68
29	-51	-56	-45	-62
30	-53	-56	-45	-65
31	-55	-49	-42	-61
32	-51	-44	-43	-63
33	-52	-48	-41	-59
Mean	**-60.21**	**-51.53**	**-42.52**	**-53.12**
Median	**-62**	**-52**	**-43**	**-52**

Appendix 3B Continue

Terminal ID AB30, Access ID MMU 2D, Monitor RAU 2N 15/85, Reception from TX19

S/N	October 2,10,22 and 28th 2009 RSL (dBm)	October5,6,7,10,15,18,19,21 and 24th 2010 RSL (dBm)
1	-50	-56
2	-49	-49
3	-52	-44
4	-51	-53
5	-51	-53
6	-53	-49
7	-44	-49
8	-51	-49
9	-51	-47
10	-51	-46
11	-53	-44
12	-48	-41
13	-54	-42
14	-56	-39
15	-49	-42
16	-44	-44
17	-44	-46
18	-50	-49
19	-49	-53
20	-52	-49
21	-51	-45
22	-49	-41

23	-51	-40
24	-53	-44
25	-54	-44
26	-55	-51
27	-51	-53
28	-52	-44
29	-49	-51
30	-48	-51
31	-48	-44
32	-49	-50
33		-49
Mean	**-50.33**	**-47.00**
Median	**-52**	**-46**

Appendix 3C

LINK DOCUMENT

	KAD008	KAD016
Elevation (m)	610.00	605.00
Latitude	10 28 31.55 N	10 30 50.00 N
Longitude	007 25 13.58 E	007 26 31.00 E
True azimuth (°)	28.96	208.96
Vertical angle (°)	0.04	-0.08
Antenna model	VHLP4-130	VHLP4-130
Antenna height (m)	40.00	50.00
Antenna gain (dBi)	42.00	42.00
Frequency (MHz)	13000.00	
Polarization	Vertical	
Path length (km)	4.86	
Free space loss (dB)	128.48	
Atmospheric absorption loss (dB)	0.10	
Field margin (dB)	1.00	
Net path loss (dB)	45.58	45.58
Radio model	SRA 4 HD-13 WB	SRA 4 HD-13 WB
TX power (watts)	0.03	0.03
TX power (dBm)	14.00	14.00
EIRP (dBm)	56.00	56.00
TX Channels	7h 13199.0000V	7l 12933.0000V
	8h 13227.0000V	8l 12961.0000V
RX threshold criteria	BER 10-3	BER 10-3
RX threshold level (dBm)	-73.50	-73.50
RX signal (dBm)	-31.58	-31.58
Thermal fade margin (dB)	41.92	41.92
Geoclimatic factor	8.86E-05	
Path inclination (mr)	1.03	
Fade occurrence factor (Po)	9.58E-04	
Average annual temperature (°C)	29.00	
Effective frequency spacing (MHz)	28.00	28.00
FD improvement factor	41.20	41.20
Worst month - multipath (%)	100.00000	100.00000
(sec)	4.02e-03	4.02e-03
Annual - multipath (%)	100.00000	100.00000
(sec)	0.02	0.02
(% - sec)	100.00000 - 0.04	
Rain region	ITU Region P	
0.01% rain rate (mm/hr)	145.00	
Flat fade margin - rain (dB)	41.92	
Rain rate (mm/hr)	230.51	
Rain attenuation (dB)	41.92	
Annual rain (% - sec)	99.99847 - 483.90	
Annual multipath + rain (% - sec)	99.99847 - 483.94	

Tue, Nov 29 2005
KAD008-KAD016_SRA 4 HD 13-1.2 VHLP 2+0 STM-1.pl4
Reliability Method - ITU-R P.530-7/8
Rain - ITU-R P.530-7

	Site ID	Station ID or IP Address	Magazine Type	Modem Type	Mounting Pole	Tx Rack
Far End	KAD016			Agile	1	
Near End	KAD008			Agile	1	
Link Configuration	1+0	Link ID	KAD008-KAD016	Polarization	Vertical	
Project Title	METRO RING					
Routing Plan	KAD008-KAD016-KAD013-KAD010-KAD008					
Prepared by	Obumneke Onwumelu					
Checked by	Festus Adefiranye					

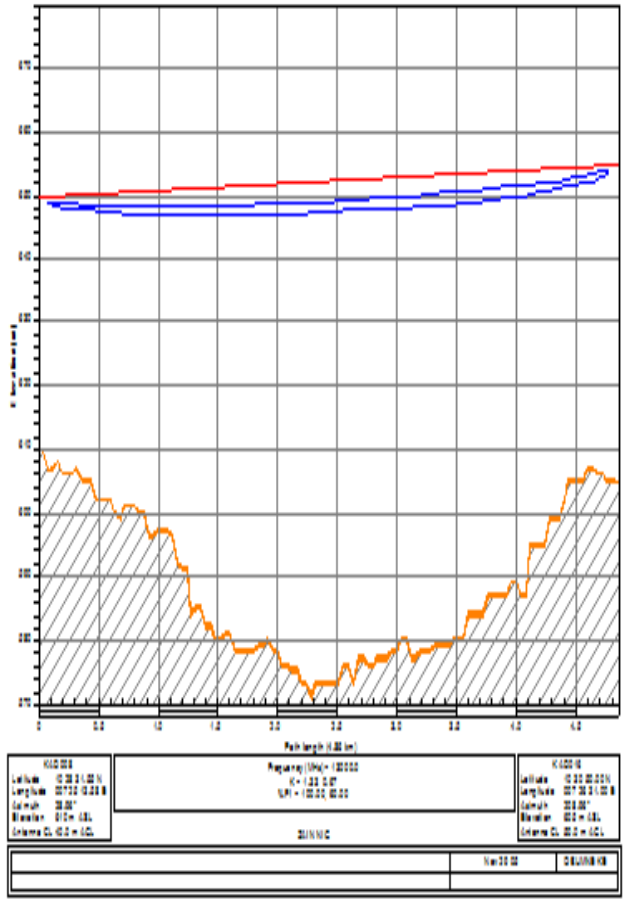

Appendix 3C Continue

	KAD010	KAD008
Elevation (m)	604.00	610.74
Latitude	10 27 05.00 N	10 28 31.49 N
Longitude	007 24 05.00 E	007 25 13.58 E
True azimuth (°)	38.12	218.13
Vertical angle (°)	0.05	-0.07
Antenna model	VHLP4-142	VHLP4-142
Antenna height (m)	40.00	37.00
Antenna gain (dBi)	42.90	42.90
Frequency (MHz)	15000.00	
Polarization	Vertical	
Path length (km)	3.38	
Free space loss (dB)	126.57	
Atmospheric absorption loss (dB)	0.09	
Field margin (dB)	1.00	
Net path loss (dB)	41.86	41.86
Radio model	SRA 4 HD-15 WB	SRA 4 HD-15 WB
TX power (watts)	0.01	0.01
TX power (dBm)	10.00	10.00
EIRP (dBm)	52.90	52.90
TX Channels	1l 14424.0000V	1h 14914.0000V
	2l 14452.0000V	2h 14942.0000V
RX threshold criteria	BER 10-3	BER 10-3
RX threshold level (dBm)	-73.00	-73.00
RX signal (dBm)	-31.86	-31.86
Thermal fade margin (dB)	41.14	41.14
Geoclimatic factor	8.86E-05	
Path inclination (mr)	1.11	
Fade occurrence factor (Po)	2.79E-04	
Average annual temperature (°C)	29.00	
Effective frequency spacing (MHz)	28.00	28.00
FD improvement factor	36.67	36.67
Worst month - multipath (%)	100.00000	100.00000
(sec)	1.55e-03	1.55e-03
Annual - multipath (%)	100.00000	100.00000
(sec)	6.98e-03	6.98e-03
(% - sec)	100.00000 - 0.01	
Rain region	ITU Region P	
0.01% rain rate (mm/hr)	145.00	
Flat fade margin - rain (dB)	41.14	
Rain rate (mm/hr)	231.67	
Rain attenuation (dB)	41.14	
Annual rain (% - sec)	99.99850 - 471.79	
Annual multipath + rain (% - sec)	99.99850 - 471.80	

Tue, Feb 03 2009
KAD010-KAD008_SRA 4 HD 15-1.2VHLP 2+0 STM-1.pl4
Reliability Method - ITU-R P.530-7/8
Rain - ITU-R P530-7

	Site ID	Station ID or IP Address	Magazine Type	Modem Type	Mounting Pole	Tx Rack
Far-End	KAD008			Agile	1	
Near-End	KAD010			Agile	1	1
Link Configuration	1+0	Link ID	KAD010-KAD008		Polarization	Vertical
Project Title	METRO RING					
Routing Plan	KAD010-KAD008-KAD016-KAD013-KAD010					
Prepared by	ObumnekeOnwumelu					
Checked by	Festus Adefiranye					

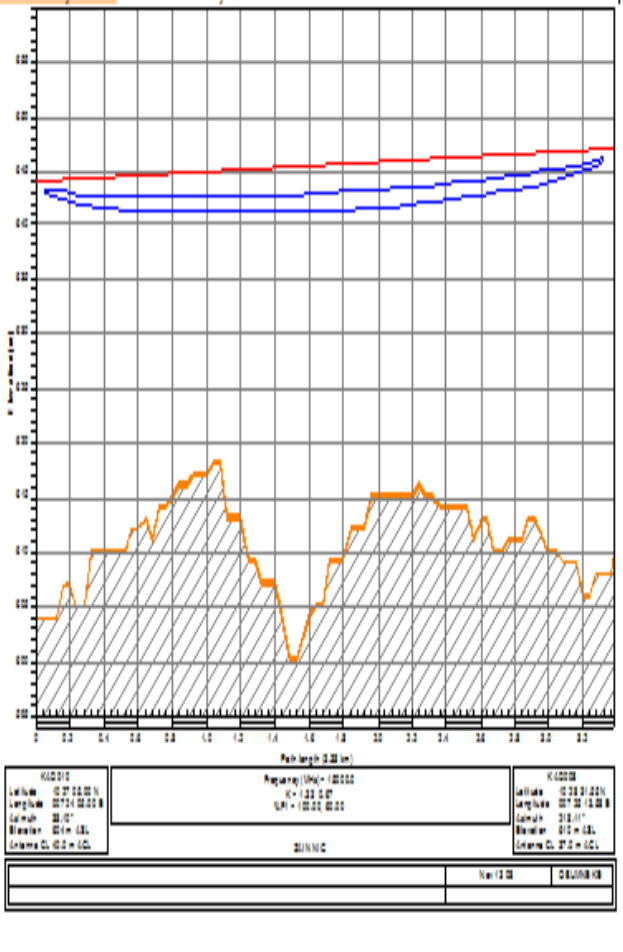

Appendix 3D

Chi-Square Distribution Table

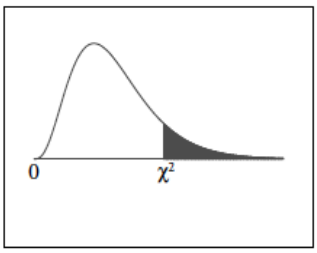

The shaded area is equal to α for $\chi^2 = \chi^2_\alpha$.

df	$\chi^2_{.995}$	$\chi^2_{.990}$	$\chi^2_{.975}$	$\chi^2_{.950}$	$\chi^2_{.900}$	$\chi^2_{.100}$	$\chi^2_{.050}$	$\chi^2_{.025}$	$\chi^2_{.010}$	$\chi^2_{.005}$
1	0.000	0.000	0.001	0.004	0.016	2.706	3.841	5.024	6.635	7.879
2	0.010	0.020	0.051	0.103	0.211	4.605	5.991	7.378	9.210	10.597
3	0.072	0.115	0.216	0.352	0.584	6.251	7.815	9.348	11.345	12.838
4	0.207	0.297	0.484	0.711	1.064	7.779	9.488	11.143	13.277	14.860
5	0.412	0.554	0.831	1.145	1.610	9.236	11.070	12.833	15.086	16.750
6	0.676	0.872	1.237	1.635	2.204	10.645	12.592	14.449	16.812	18.548
7	0.989	1.239	1.690	2.167	2.833	12.017	14.067	16.013	18.475	20.278
8	1.344	1.646	2.180	2.733	3.490	13.362	15.507	17.535	20.090	21.955
9	1.735	2.088	2.700	3.325	4.168	14.684	16.919	19.023	21.666	23.589
10	2.156	2.558	3.247	3.940	4.865	15.987	18.307	20.483	23.209	25.188
11	2.603	3.053	3.816	4.575	5.578	17.275	19.675	21.920	24.725	26.757
12	3.074	3.571	4.404	5.226	6.304	18.549	21.026	23.337	26.217	28.300
13	3.565	4.107	5.009	5.892	7.042	19.812	22.362	24.736	27.688	29.819
14	4.075	4.660	5.629	6.571	7.790	21.064	23.685	26.119	29.141	31.319
15	4.601	5.229	6.262	7.261	8.547	22.307	24.996	27.488	30.578	32.801
16	5.142	5.812	6.908	7.962	9.312	23.542	26.296	28.845	32.000	34.267
17	5.697	6.408	7.564	8.672	10.085	24.769	27.587	30.191	33.409	35.718
18	6.265	7.015	8.231	9.390	10.865	25.989	28.869	31.526	34.805	37.156
19	6.844	7.633	8.907	10.117	11.651	27.204	30.144	32.852	36.191	38.582
20	7.434	8.260	9.591	10.851	12.443	28.412	31.410	34.170	37.566	39.997
21	8.034	8.897	10.283	11.591	13.240	29.615	32.671	35.479	38.932	41.401
22	8.643	9.542	10.982	12.338	14.041	30.813	33.924	36.781	40.289	42.796
23	9.260	10.196	11.689	13.091	14.848	32.007	35.172	38.076	41.638	44.181
24	9.886	10.856	12.401	13.848	15.659	33.196	36.415	39.364	42.980	45.559
25	10.520	11.524	13.120	14.611	16.473	34.382	37.652	40.646	44.314	46.928
26	11.160	12.198	13.844	15.379	17.292	35.563	38.885	41.923	45.642	48.290
27	11.808	12.879	14.573	16.151	18.114	36.741	40.113	43.195	46.963	49.645
28	12.461	13.565	15.308	16.928	18.939	37.916	41.337	44.461	48.278	50.993
29	13.121	14.256	16.047	17.708	19.768	39.087	42.557	45.722	49.588	52.336
30	13.787	14.953	16.791	18.493	20.599	40.256	43.773	46.979	50.892	53.672
40	20.707	22.164	24.433	26.509	29.051	51.805	55.758	59.342	63.691	66.766
50	27.991	29.707	32.357	34.764	37.689	63.167	67.505	71.420	76.154	79.490
60	35.534	37.485	40.482	43.188	46.459	74.397	79.082	83.298	88.379	91.952
70	43.275	45.442	48.758	51.739	55.329	85.527	90.531	95.023	100.425	104.215
80	51.172	53.540	57.153	60.391	64.278	96.578	101.879	106.629	112.329	116.321
90	59.196	61.754	65.647	69.126	73.291	107.565	113.145	118.136	124.116	128.299
100	67.328	70.065	74.222	77.929	82.358	118.498	124.342	129.561	135.807	140.169

Appendix 3E

MatlabSimulationProgram

```
f=figure('name', 'SIMULATION OF THE EFFECTS OF RAIN DROPS ON 13GHz and
15GHz links');
% Mean Rain rates of Kaduna for% 13GHz link and 15GHz
     Rp=[12.325 17.06 30.58 23.43 39.095 27.3 21.615];
% Measured rain attenuation of Kaduna for 13GHz link and 15GHz link
     Am_13=[2.72 4.09 8.78 4.52 9.89 8.75 5.82];
     Am_15=[3.52 6.15 15.42 10.42 17.52 12.32 11.25];
% Iteration calculating the predicted mean attenuation of Kaduna
for i=1:7
     Ap_13(i)= -0.0038*Rp(i)^2+0.4878*Rp(i)-3.0414;
     Ap_15(i)= -0.0107*Rp(i)^2+1.084*Rp(i)-8.4759;

% Calculation of error in the measurements of rain attenuation
     err_13(i)=Am_13(i)-Ap_13(i);
     err_15(i)=Am_15(i)-Ap_15(i);
end
% Mean model error
     MME_13 = mean(err_13);
     MME_15 = mean(err_15);

% Standard deviation
     SD_13=sqrt(1/7*(sum(err_13)- mean(err_13))^2);
     SD_15=sqrt(1/7*(sum(err_15)- mean(err_15))^2);

% Coefficient of correlation
     N= 7;
     R = sum (Rp);
     A_13=sum(Ap_13);
     A_15=sum(Ap_15);

     Rpav =R/N;
     Ap_13av=A_13/N;
     Ap_15av=A_15/N;
     r_13 = sum((R-Rpav)*(A_13-Ap_13av))/sqrt((sum(R-
Rpav)^2)*(sum(A_13-Ap_13av)^2));
     r_15 = sum((R-Rpav)*(A_15-Ap_15av))/sqrt((sum(R-
Rpav)^2)*(sum(A_15-Ap_15av)^2));
% Calculation of mean standard error
     MSE_13=SD_13/sqrt(N);
     MSE_15=SD_15/sqrt(N);


% Root mean standard error
     RMSE_13=sqrt(MSE_13);
     RMSE_15=sqrt(MSE_15);
     fprintf('The predicted attenuation, Ap_13=%4.2f dB\n',Ap_13)
     fprintf('The predicted attenuation, Ap_15=%4.2f dB\n',Ap_15)
     fprintf('The rain rate, Rp=%4.3f mm/h\n',Rp)
     fprintf('The Measured attenuation, Am_13=%4.2f dB\n',Am_13)
```

Appendix 3E (Continue)

```
    fprintf('The Measured attenuation, Am_15=%4.2f dB\n',Am_15)
    fprintf('The model error, err_13=%4.2f dB\n',err_13)
    fprintf('The model error, err_15=%4.2f dB\n',err_15)
    fprintf('MSE_13 is %4.4f\n',MSE_13)
    fprintf('MSE_15 is %4.4f\n',MSE_15)
    fprintf('RMSE_13 is %4.4f\n',RMSE_13)
    fprintf('RMSE_15 is %4.4f\n',RMSE_15)
    fprintf('Mean model error_13 =%4.5f\n',MME_13)
    fprintf('Mean model error_15 =%4.5f\n',MME_15)
    fprintf('R is %4.4f\n',R)
    fprintf('SD_13 is %4.4f\n',SD_13)
    fprintf('SD_15 is %4.4f\n',SD_15)
    fprintf('coefficient of correlation_13 is %4.4f\n',r_13)
    fprintf('coefficient of correlation_15 is %4.4f\n',r_15)
%%%%%%%%%%%%%%%%%%%%%%%%%%%%%%%%%%%%%%%%%%%%%%%%%%%%%%%%%%%%%%%%%%%%%%%
%%%%%%%%%%%%%%%
    coef_13=polyfit(Rp,Ap_13,1);
    fprintf('Gradient of Predicted Model at 13GHz is
%4.4f\n',coef_13(1));
    fprintf('Y intercept of Predicted Model at 13GHz is
%4.4f\n',coef_13(2));
%%%%%%%%%%%%%%%%%%%%%%%%%%%%%%%%%%%%%%%%%%%%%%%%%%%%%%%%%%%%%%%%%%%%%%%
%%%%%%%%%%%%%%%%%
    subplot(2,1,1),plot(Rp,Am_13,'-redo',Rp,Ap_13,'-
blue+','linewidth',2)
    xlabel('rain rate in mm/h')
    ylabel('Attenuation in dB')
    legend('Measured attenuation','Simulated attenuation')
    title('The Measured and Simulated attenuation (dB) for 13GHz
link')
    hold on
    grid on
%%%%%%%%%%%%%%%%%%%%%%%%%%%%%%%%%%%%%%%%%%%%%%%%%%%%%%%%%%%%%%%%%%%%%%%
%
    coef_15=polyfit(Rp,Ap_15,1);
    fprintf('Gradient of Predicted Model at 15GHz is
%4.4f\n',coef_15(1));
    fprintf('Y intercept of Predicted Model at 15GHz is
%4.4f\n',coef_15(2));
%%%%%%%%%%%%%%%%%%%%%%%%%%%%%%%%%%%%%%%%%%%%%%%%%%%%%%%%%%%%%%%%%%%%%%%
%%%%%%%%%%%%
    subplot(2,1,2),plot(Rp,Am_15,'-redo',Rp,Ap_15,'-
blue+','linewidth',2)
    xlabel('rain rate in mm/h')
    ylabel('Attenuation in dB')
    legend('Measured attenuation','Simulated attenuation')
    title('The Measured and Simulated attenuation (dB) for 15GHz
link')
    hold on
    grid on
```

Appendix 4A

Comparison of the Developed Model with ITU-R Model

2010

```
clc;
clearall;
closeall;
x=linspace(1,7,7);
Predicted_13Ghz=[4.64 4.90 9.62 8.13 8.74 9.43 5.65];
Attenuation_13Ghz_A0_1=[1.74 1.80 3.31 2.76 2.97 3.23 2.00];
Attenuation_13Ghz_A0_01=[4.56 4.71 8.66 7.22 7.77 8.46 5.24];
Attenuation_13Ghz_A0_001=[9.73 10.05 18.49 15.40 16.58 18.05 11.18];
%=========================================================================
Predicted_15Ghz=[7.85 8.36 16.74 14.37 15.38 16.46 9.82];
Attenuation_15Ghz_A0_1=[2.34 2.41 4.34 3.64 3.91 4.24 2.67];
Attenuation_15Ghz_A0_01=[6.12 6.31 11.37 9.53 10.23 11.11 6.99];
Attenuation_15Ghz_A0_001=[13.06 13.47 24.26 20.34 21.85 23.71 14.93];
figure('Name','GRAPH OF ATTENUATION FOR 13GHZ','NumberTitle','off');
%bar(Attenuation_13Ghz);
plot(x,Predicted_13Ghz,'-+r',x,Attenuation_13Ghz_A0_1,'-
.ok',x,Attenuation_13Ghz_A0_01,'--*b',x,Attenuation_13Ghz_A0_001,'-
g','LineWidth',2);
legend('PREDICTED ATTN','0.1% ITU ATTN','0.01% ITU ATTN','0.001% ITU
ATTN','Location','Best');
set(gca,'XTickLabel','APR|MAY|JUN|JUL|AUG|SEPT|OCT');
gridon;
ylabel('Rain Attenuation');
xlabel('Gregorian calendar months');
title('PREDICTED 13 GHz ATTN WITH ITU-R CALCULATED AT 0.1, 0.01 AND
0.001% 2010');
%line(Attenuation_13Ghz,'LineWidth',4,'Color',[.8 .8 .8]);
figure('Name','GRAPH OF ATTENUATION FOR 15GHZ','NumberTitle','off');
plot(x,Predicted_15Ghz,'-+r',x,Attenuation_15Ghz_A0_1,'-
.ok',x,Attenuation_15Ghz_A0_01,'--*b',x,Attenuation_15Ghz_A0_001,'-
g','LineWidth',2);
set(gca,'XTickLabel','APR|MAY|JUN|JUL|AUG|SEPT|OCT');
legend('PREDICTED ATTN','0.1% ITU ATTN','0.01% ITU ATTN','0.001% ITU
ATTN','Location','Best');
gridon;
ylabel('Rain Attenuation');
xlabel('Gregorian calendar months');
title('PREDICTED 15 GHz ATTN WITH ITU-R CALCULATED AT 0.1, 0.01 AND
0.001% 2010');
```

2009

```
clc;
clearall;
closeall;
x=linspace(1,7,7);
Predicted_13Ghz=[0.18 3.42 6.79 4.16 11.35 4.98 5.81];
Attenuation_13Ghz_A0_1=[0.61 1.42 2.33 1.61 4.17 1.82 2.05];
Attenuation_13Ghz_A0_01=[1.59 3.73 6.10 4.21 10.91 4.77 5.35];
Attenuation_13Ghz_A0_001=[3.39 7.96 13.02 8.98 23.29 10.18 11.43];
```

Appendix 4A (Continue)

```
%=========================================================================
Predicted_15Ghz=[2.20 5.38 11.98 6.88 18.78 8.53 10.12];
Attenuation_15Ghz_A0_1=[0.84 1.92 3.10 2.16 5.53 2.44 2.73];
Attenuation_15Ghz_A0_01=[2.21 5.04 8.10 5.66 14.21 6.39 7.14];
Attenuation_15Ghz_A0_001=[4.72 10.75 17.29 12.09 30.33 13.64 15.25];
figure('Name','GRAPH OF ATTENUATION FOR 13GHZ','NumberTitle','off');
%bar(Attenuation_13Ghz);
plot(x,Predicted_13Ghz,'-+r',x,Attenuation_13Ghz_A0_1,'-
.ok',x,Attenuation_13Ghz_A0_01,'--*b',x,Attenuation_13Ghz_A0_001,'-
g','LineWidth',2);
legend('PREDICTED ATTN','0.1% ITU ATTN','0.01% ITU ATTN','0.001% ITU
ATTN','Location','Best');
set(gca,'XTickLabel','APR|MAY|JUN|JUL|AUG|SEPT|OCT');
gridon;
ylabel('Rain Attenuation');
xlabel('Gregorian calendar months');
title('PREDICTED 13 GHz ATTN WITH ITU-R CALCULATED AT 0.1, 0.01 AND
0.001% 2009');
%line(Attenuation_13Ghz,'LineWidth',4,'Color',[.8 .8 .8]);
figure('Name','GRAPH OF ATTENUATION FOR 15GHZ','NumberTitle','off');
plot(x,Predicted_15Ghz,'-+r',x,Attenuation_15Ghz_A0_1,'-
.ok',x,Attenuation_15Ghz_A0_01,'--*b',x,Attenuation_15Ghz_A0_001,'-
g','LineWidth',2);
set(gca,'XTickLabel','APR|MAY|JUN|JUL|AUG|SEPT|OCT');
legend('PREDICTED ATTN','0.1% ITU ATTN','0.01% ITU ATTN','0.001% ITU
ATTN','Location','Best');
gridon;
ylabel('Rain Attenuation');
xlabel('Gregorian calendar months');
title('PREDICTED 15 GHz ATTN WITH ITU-R CALCULATED AT 0.1, 0.01 AND
0.001% 2009');
```